

## Slepton Production as a Probe of the Squark Mass Scale

Mihoko M. Nojiri,<sup>a</sup> Damien M. Pierce,<sup>b</sup> and Youichi Yamada<sup>c</sup>

<sup>a</sup> *KEK Theory Group, Oho 1-1, Tsukuba, Ibaraki, 305 Japan*

<sup>b</sup> *Stanford Linear Accelerator Center, Stanford University, Stanford, California 94309, USA*

<sup>c</sup> *Department of Physics, Tohoku University, Sendai, 980-77, Japan*

### Abstract

We investigate an important radiative correction to the slepton and chargino production processes. We consider a supersymmetric spectrum with a large splitting between the squark and slepton masses. In this case, in the effective theory below the squark mass threshold, the supersymmetric Slavnov-Taylor identities which enforce the equality of the gauge and gaugino couplings are violated. The gaugino propagators receive potentially large corrections due to virtual quark/squark loop effects. We compute the full one-loop (s)quark corrected slepton production cross-sections. The  $t$ -channel one-loop scattering amplitudes are factorized into an effective chargino/neutralino mass matrix and an effective fermion-sfermion-gaugino coupling. The difference between the effective gaugino coupling and the gauge coupling is proportional to  $\log(M_{\tilde{Q}}/m_{\tilde{\ell}})$  in the large squark mass limit. We find that the one-loop corrected slepton production cross-sections can depend on the squark mass strongly, up to  $9\% \times \log_{10}(M_{\tilde{Q}}/m_{\tilde{\ell}})$ . We investigate the squark mass sensitivity of the slepton cross-section measurements at a future linear collider. For sneutrino production accessible at  $\sqrt{s} = 500$  GeV there can be sensitivity to squark masses at or larger than 1 TeV.

*D.M.P. is supported by Department of Energy contract DE-AC03-76SF00515. M.M.N. is supported in part by Grant in aid for Science and Culture of Japan (07640428, 09246232), and JSPS Japanese-German Cooperative Science Program.*

# 1 Introduction

Supersymmetry is an attractive possibility beyond the standard model. Because of the relations supersymmetry imposes among the dimensionless couplings, the quadratic divergences in the Higgs sector are cut-off by the superpartner mass scale. The cancellations stabilize the hierarchy between the Planck scale and the weak scale. The minimal supersymmetric standard model (MSSM) is consistent with gauge coupling unification suggested by grand unified theories. Also, it is interesting that one of the hallmarks of supersymmetry, a light Higgs boson ( $m_h \lesssim 130$  GeV), is favored by global fits to precision electroweak data [1].

If low energy supersymmetry exists, superpartners will be copiously produced at the next generation of supercolliders. For example, the Large Hadron Collider (LHC) could produce thousands of gluino pairs in a single day. Each gluino would then, in a typical scenario, decay to the lightest supersymmetric particle (LSP) through a cascade of charginos, neutralinos, jets and leptons. Detailed information about the superpartner masses can be determined from such processes [2]. A future Linear Collider (LC) would likewise prove to be an invaluable tool in measuring the parameters of the soft-supersymmetry breaking Lagrangian, as precision measurements of the superpartner spectrum, cross-sections, and branching ratios are possible [3, 4, 5, 6, 7, 8]. The constrained kinematics, tunable center-of-mass energy, and beam polarization allow for direct and model independent interpretations of the measurements. Also, in many processes the backgrounds are quite small.

In this paper we examine the prospect of testing supersymmetry via a precise measurement of the lepton-slepton-gaugino vertex. The linear collider provides a suitably clean experimental environment. Among the relations which account for the cancellations of quadratic divergences, supersymmetry relates the lepton-slepton-gaugino coupling to the usual gauge coupling.

Although bare (or  $\overline{\text{DR}}$ ) couplings enjoy the relations imposed by supersymmetry, the effective gauge and gaugino couplings are not equal because supersymmetry is broken. In particular, all non-singlet nondegenerate supermultiplets such as the quark-squark supermultiplets contribute to the splitting. Even arbitrarily heavy split multiplets will contribute, although the contribution will be suppressed by the heavy mass scale. Hence, measurements of the type we consider here not only provide for detailed tests of supersymmetry, but can also elucidate important features of the scale and pattern of supersymmetry breaking [9, 10, 11, 12].

For example, the (s)quark contribution to the splitting of the U(1) and SU(2) gaugino/gauge (s)lepton couplings grows logarithmically with the squark mass, as

$$\frac{\delta g_Y}{g_Y} \simeq \frac{11g_Y^2}{48\pi^2} \ln \left( \frac{M_{\tilde{Q}}}{m_{\tilde{\ell}}} \right), \quad \frac{\delta g_2}{g_2} \simeq \frac{3g_2^2}{16\pi^2} \ln \left( \frac{M_{\tilde{Q}}}{m_{\tilde{\ell}}} \right). \quad (1)$$

This correction is obtained by evolving the couplings according to the renormalization group equations (RGE's) of the effective theory [13] below the squark mass threshold. When  $M_{\tilde{Q}}/m_{\tilde{\ell}} \simeq 10$  the correction to the SU(2) (U(1)) coupling is about 2% (0.7%). This gives rise to an enhancement of the  $t$ -channel slepton or gaugino production cross-section of about 8% (2.8%). If large statistics are available and systematic errors can be controlled, we can (assuming the MSSM) constrain the squark mass scale by this measurement. Notice that a modest hierarchy between the squark and slepton masses is typical of the simplest gauge mediated models, which predict  $M_{\tilde{Q}}/m_{\tilde{\ell}_R} \simeq 6$ .

As another example, it has been proposed that the scalar masses of the first two generations might be very heavy (e.g. 20 TeV) so that the FCNC constraints on the scalar masses are alleviated [14]. This large hierarchy in the superpartner spectrum will be reflected in the splitting of the gaugino/gauge couplings of the third generation (s)fermions.

We restrict our attention to the measurement of the first generation lepton-slepton-gaugino coupling at an  $e^-e^+$  linear collider. Much study has been undertaken to determine how accurately we can expect to measure these couplings. Two relevant processes to consider are chargino production and slepton production. These processes involve the lepton-slepton-gaugino coupling by way of the  $t$ -channel exchange of a sfermion or gaugino. The measurement of the gaugino coupling via the chargino production process has been considered in Ref. [5]. In that study the authors worked under the assumption that only chargino production was available. It was shown that the  $\tilde{W}\tilde{\nu}_e e_L$  coupling could be determined to about 20%. Incorporating knowledge about the sneutrino mass allows for an improved  $\mathcal{O}(2\text{-}3\%)$  determination of the  $\tilde{W}\tilde{\nu}_e e_L$  coupling [10]. A more precise determination is possible by studying slepton production. In Ref. [8] it was demonstrated that by measuring  $\tilde{e}_R^-\tilde{e}_R^+$  production the U(1)  $\tilde{B}\tilde{e}e$  coupling could be determined to about 1%. Note that this is the same order of magnitude as the splitting due to heavy squarks (see Eq. (1)). In Ref. [10] it was estimated that a  $\mathcal{O}(0.3\%)$  measurement of the U(1) gaugino coupling could be achieved by measuring  $\tilde{e}_R^-\tilde{e}_R^-$  production at an  $e^-e^-$  collider.

We perform a full one-loop calculation of the slepton production cross-section within the MSSM. Since we are interested in the sensitivity to the squark mass scale, we assume the squark mass spectrum is well approximated by a single mass scale,  $M_{\tilde{Q}}$ , and allow for a large hierarchy between the squark and slepton masses. We include only (s)quark loops in the calculation, because the correction is enhanced by a color factor and the number of generations. The remaining corrections are small, and if we did include them we expect our conclusions would not change.

In the next section we discuss the radiative correction calculation. We point out that, to a good approximation, the one-loop  $t$ -channel amplitudes can be rewritten in the same form as the tree-level amplitudes, with the replacement of the tree-level parameters with renormalized effective parameters. Hence we introduce the effective coupling, the effective masses, and the effective mixing matrix. In section 3 we show our numerical results. We show the renormalization scale and squark mass dependence of the various production modes, for the different electron polarizations. We compare the tree-level, leading-log, effective, and full cross-section calculations. The results show that the effective theory approximation describes the full result very well. We also discuss the  $A$ -term dependence.

In section 4 we discuss how well we can measure the squark loop correction to the coupling, and thereby constrain the squark mass, assuming both slepton and chargino production are possible. We show the statistical significance of the results by combining our knowledge of the superpartner masses and cross-sections. The slepton production cross-section is a sensitive function of the slepton mass. The uncertainty in the slepton mass measurement is quite important in this analysis. We emphasize that the chargino production cross-section does not have this problem of the final-state mass uncertainty. In the last section, section 5, we give our conclusions.

## 2 The one-loop cross-section

In this section we discuss the calculation of the cross-section of  $e^-e^+ \rightarrow \tilde{\ell}_i\tilde{\ell}_j^*$ , where  $\tilde{\ell}_i = (\tilde{e}_L^-, \tilde{e}_R^-, \tilde{\nu}_e)$ , including one-loop (s)quark corrections. The full result is explicitly given in Appendix A; here we restrict ourselves to outline the general features of the calculation.

As a specific example, we consider the process  $e^-e^+ \rightarrow \tilde{e}_R\tilde{e}_R^*$ . The tree-level amplitude is given by

$$\mathcal{M}_{RR}^{(0)} = 2\bar{v}\not{p}\left[\frac{e^2}{s} + \frac{g_Y^2}{s - M_Z^2}\left(s_W^2 - \frac{1}{2}P_L\right) - \sum_{i=1}^4 \frac{g_Y^2 N_{i1}^* N_{i1}}{p^2 - m_{\tilde{\chi}_i^0}^2} P_R\right]u, \quad (2)$$

where  $s$  is the center-of-mass energy,  $p$  is the  $t$ -channel momentum, and  $P_{L,R} = (1 \mp \gamma_5)/2$ . The sine of the weak mixing angle is denoted  $s_W$ ,  $N_{ij}$  is the neutralino mixing matrix, and the  $e^\pm$  wave functions are denoted  $\bar{v}$  and  $u$ .

To evaluate the one-loop amplitude, we treat all the parameters appearing in this tree-level expression as running  $\overline{\text{DR}}$  (dimensional reduction with modified minimal subtraction [15]) quantities, and add the contributions from the one-loop diagrams (see Fig. 1). Note that the (s)quark loop corrections do not give rise to external wave-function renormalization.

We take the gauge boson pole masses and the standard model  $\overline{\text{MS}}$  electromagnetic coupling  $\hat{\alpha}_{\text{SM}}(M_Z)$  as inputs. The  $\overline{\text{DR}}$  parameters are related to the corresponding input parameters by familiar expressions. (Hatted symbols are  $\overline{\text{DR}}$  renormalized quantities. We do not hat the  $\overline{\text{DR}}$  soft supersymmetry breaking parameters.) For example, the running gauge boson masses are given by

$$\hat{M}_W^2(Q) = M_W^2 + \mathcal{R}e \hat{\Pi}_{WW}^T(M_W^2), \quad \hat{M}_Z^2(Q) = M_Z^2 + \mathcal{R}e \hat{\Pi}_{ZZ}^T(M_Z^2), \quad (3)$$

where the  $\hat{\Pi}^T$  are the transverse parts of the  $\overline{\text{DR}}$  renormalized gauge-boson self-energies. The gauge coupling in the full theory  $\hat{e}(Q)$  is related to that of the effective theory (i.e. the standard model in the  $\overline{\text{MS}}$  scheme) as <sup>1</sup>

$$\hat{e}(Q) = \hat{e}_{\text{SM}}(Q) \left( 1 + \frac{\hat{e}_{\text{SM}}^2 N_c}{48\pi^2} \sum_{\tilde{q}_i} Q_{\tilde{q}_i}^2 \ln \frac{Q}{m_{\tilde{q}_i}} \right). \quad (4)$$

The  $\text{SU}(2)_L$  and  $\text{U}(1)_Y$  gauge couplings are then obtained in terms of the gauge boson running masses,

$$\hat{g}_Y^2(Q) = \hat{e}^2(Q) \frac{\hat{M}_Z^2}{\hat{M}_W^2}, \quad (5)$$

$$\hat{g}_2^2(Q) = \hat{e}^2(Q) \frac{\hat{M}_Z^2}{\hat{M}_Z^2 - \hat{M}_W^2}. \quad (6)$$

Note that the argument of the gauge-boson self-energies is the external momentum squared. They implicitly depend on the renormalization scale  $Q$ . Explicit expressions for  $\hat{\Pi}_{WW,ZZ}^T$  are given in [16, 17]. Since we only include the (s)quark loop corrections, for consistency the  $\overline{\text{DR}}$  parameters only run by virtue of the (s)quark contributions to their RGE's.

<sup>1</sup>The constant term ( $e^2/24\pi^2$ ) for  $\overline{\text{MS}}$  to  $\overline{\text{DR}}$  conversion is omitted because we systematically ignore the gauge boson loops.

When  $M_1$ ,  $M_2$ ,  $\mu$ ,  $\tan\beta$  are needed, we use  $M_1(M_1)$ ,  $M_2(M_2)$ ,  $\mu(|\mu|)$ ,  $\tan\beta(M_Z)$ . The scale choice of each parameters has been made because the relations  $m_{\tilde{\chi}_1^0} \simeq M_1(M_1)$ ,  $m_{\tilde{\chi}_2^0} \simeq M_2(M_2)$ ,  $m_{\tilde{\chi}_3^0} \simeq |\mu|$  hold when  $\max(M_1, M_2, |\mu|) \gg M_Z$ , and  $M_{\tilde{q}_i} \lesssim \min(M_1, M_2, |\mu|)$ .

With these counter-terms and the one-loop diagram contributions presented in Appendix A, we obtain the full one-loop amplitude. The differential cross-section is then computed,

$$\frac{d\sigma}{dt} = \frac{1}{16\pi s^2} |\mathcal{M}|^2 . \quad (7)$$

To obtain the total cross-section, we integrate over the  $t$ -channel momentum numerically. The cross-sections for the other selectron and sneutrino production processes are obtained similarly.

In Appendix B, we show how the one-loop corrected  $t$ -channel amplitude can be well approximated by a tree-level form,

$$\mathcal{M}_{RR}^t = 2\bar{v}\not{p} \left[ - \sum_{i=1}^4 \frac{\bar{g}_{e\tilde{e}_R\tilde{B}}^2 \bar{N}_{i1}^* \bar{N}_{i1}(p^2)}{p^2 - \bar{m}_i^2(p^2)} P_R \right] u , \quad (8)$$

where  $\bar{g}_{e\tilde{e}_R\tilde{B}}(p^2)$  is the effective bino coupling defined as

$$\bar{g}_{e\tilde{e}_R\tilde{B}}(p^2) = \hat{g}_Y(Q^2) \left( 1 - \frac{1}{2} \tilde{\Sigma}_{11}^L(p^2) \right) , \quad (9)$$

and  $\tilde{\Sigma}_{11}^L(p^2)$  is the bino-bino component of the neutralino two-point function defined in Eq. (B.4). The  $\bar{N}_{ij}$  and  $\bar{m}_i$  are the effective neutralino mixing matrix and neutralino masses obtained by diagonalizing the effective neutralino mass matrix  $\bar{Y}_{ij}$ , defined in Eq. (B.6). We note that  $\bar{m}_i(\bar{m}_i^2)$  are the chargino and neutralino pole masses. Also,  $\bar{g}_i$ ,  $\bar{N}_{ij}$ , and  $\bar{m}_i$  are scale independent quantities to  $\mathcal{O}(\alpha)$ . For example, the scale dependence of  $\hat{g}_Y(Q)$  is cancelled by the implicit scale dependence of  $\tilde{\Sigma}_{11}^L(p^2)$ .

The physical correction appears as a violation of the tree-level relation  $\bar{g}_{\ell\tilde{\ell}\tilde{\chi}} = \hat{g}^{\text{eff}}$ , where  $\hat{g}^{\text{eff}}$  is the effective coupling in the standard model. It is obtained by Eqs. (3-6), including only quark contributions in the self-energies. The  $\log M_{\tilde{Q}}$  terms in  $\bar{g}_{\ell\tilde{\ell}\tilde{\chi}} - \hat{g}$  and  $\hat{g}^{\text{eff}} - \hat{g}$  correspond to the change in the beta functions above and below the squark threshold. Also, the leading logarithms of the corrections  $\delta g/g = (\bar{g}_{\ell\tilde{\ell}\tilde{\chi}} - \hat{g}^{\text{eff}})/\hat{g}^{\text{eff}}$  at  $Q = m_{\tilde{\ell}}$  are exactly those of Eq. 1, showing that the RGE approach of Ref. [13] gives the proper results.

The other effective couplings  $\bar{g}_{e\tilde{e}_L\tilde{B}}$ ,  $\bar{g}_{e\tilde{e}_L\tilde{W}}$  and  $\bar{g}_{e\tilde{\nu}_e\tilde{W}}$  are given by analogous formulae (see Eq. (B.11)). The expressions for  $\bar{g}_{e\tilde{e}_L\tilde{W}}$  and  $\bar{g}_{e\tilde{\nu}_e\tilde{W}}$  are different. However, they approach each other in the large  $M_{\tilde{Q}}$  limit. The difference between these effective couplings arises from finite electroweak symmetry breaking contributions proportional to the vacuum expectation value of the Higgs bosons. By gauge symmetry, the leading  $\log M_{\tilde{Q}}$  correction is the same for the different effective couplings. In section 3, we will see that the various finite corrections are not large compared to the leading  $\log M_{\tilde{Q}}$  correction.

In contrast to the  $t$ -channel amplitudes, the squark corrections to the  $s$ -channel amplitudes are proportional to  $(M_Z^2 \text{ or } m_t^2)/M_{\tilde{Q}}^2$ . Since we take as inputs the standard model coupling, and the  $W$ - and  $Z$ -boson pole masses, the decoupling theorem applies, and the effect of the heavy squarks is negligible in the large squark mass limit.

Part of the radiative corrections we are considering are closely related to the corrections to the neutralino and chargino masses [17, 18]. Since the chargino and neutralino masses will be measured in future collider experiments, we will in some of the discussion take the pole masses  $m_{\tilde{\chi}_1^0}$ ,  $m_{\tilde{\chi}_1^+}$ ,  $m_{\tilde{\chi}_3^0}$  as inputs.

We define  $M_1^{\text{eff}}$ ,  $M_2^{\text{eff}}$ ,  $-\mu^{\text{eff}}$  as the (1,1), (2,2), and (3,4) components of the effective neutralino mass matrix  $\bar{Y}_N$ .  $M_2^{\text{eff}}$  and  $\mu^{\text{eff}}$  could also be defined as the (1,1), (2,2) components of the effective chargino mass matrix  $\bar{Y}_C$ . These definitions differ by  $\mathcal{O}(M_Z^2/\max(M_1^2, M_2^2, \mu^2))$ , as do the different definitions of the wino effective couplings. The grand unification condition leads to the one-loop relations  $M_1/\alpha_1 = M_2/\alpha_2 = M_3/\alpha_3$ . We comment that there is a  $\ln M_{\tilde{Q}}$  correction to the  $M_i^{\text{eff}}/\alpha_i^{\text{eff}}$  ratios. We set  $M_2 \sim 2M_1$ , but we do not impose any such relation in our analysis.

### 3 Numerical results

We next study the numerical dependence of the one-loop corrected cross-sections of  $e^-e^+ \rightarrow \tilde{\ell}_i\tilde{\ell}_j^*$  ( $\tilde{\ell}_i = (\tilde{e}_L^-, \tilde{e}_R^-, \tilde{\nu}_e)$ ) on the squark mass. We consider the case where the initial electron is completely longitudinally polarized. We therefore treat the following eight modes,

$$\begin{aligned} e_L^-e^+ &\rightarrow \tilde{e}_L^-\tilde{e}_L^+, \tilde{e}_R^-\tilde{e}_R^+, \tilde{e}_L^-\tilde{e}_R^+, \tilde{\nu}_e\tilde{\nu}_e^*, \\ e_R^-e^+ &\rightarrow \tilde{e}_L^-\tilde{e}_L^+, \tilde{e}_R^-\tilde{e}_R^+, \tilde{e}_R^-\tilde{e}_L^+, \tilde{\nu}_e\tilde{\nu}_e^*. \end{aligned} \quad (10)$$

In the squark sector, we set

$$M_{\tilde{Q}} = M_{\tilde{U}} = M_{\tilde{D}}, \quad A \equiv A_t/M_{\tilde{Q}} = A_b/M_{\tilde{Q}}, \quad (11)$$

where  $M_{\tilde{Q}}$ ,  $M_{\tilde{U}}$ , and  $M_{\tilde{D}}$  are the soft-breaking masses of the left-handed, right-handed up, and right-handed down-type squarks, respectively, and  $A_t$ ,  $A_b$  are the soft-breaking Higgs-squark-squark trilinear couplings, in the convention of Ref. [19]. We assume generation independence for these parameters.

The renormalization scale independence of the one-loop cross-section serves as an important check of the calculation. In Fig. 2 we show the  $Q$  dependence of the tree-level cross-sections (defined as the first terms of Eqs. (A.4–A.8)) and the corrected ones, for  $M_1(M_1) = 100$  GeV,  $M_2(M_2) = 200$  GeV,  $\mu(|\mu|) = -300$  GeV,  $\tan\beta(M_Z) = 4$ ,  $m_{\tilde{t}} = 200$  GeV,  $M_{\tilde{Q}} = 1000$  GeV, and  $\sqrt{s} = 500$  GeV. The tree-level cross-sections vary linearly with  $\log Q$ . This dependence is due to the running of  $\hat{g}_i(Q)$ ,  $\hat{M}_Z$ , and  $M_i(Q)$ . One can see that this  $Q$  dependence almost vanishes after the inclusion of the one-loop contributions. The remaining  $Q$  dependence of the corrected cross-sections, which comes from residual higher-order corrections in the numerical calculation, is very small for  $M_Z < Q < 1$  TeV. The renormalization scale dependence suggests the uncertainty in the calculation due to higher order corrections.

We next consider the squark mass dependence of the corrected cross-sections. As stated, we take the standard model electromagnetic coupling and the  $W$  and  $Z$  boson pole masses as inputs. Here we also take the three pole masses ( $m_{\tilde{\chi}_1^0}$ ,  $m_{\tilde{\chi}_1^+}$ ,  $m_{\tilde{\chi}_3^0}$ ), and  $\tan\beta(M_Z)$  as inputs. We assume  $|\mu| \gg M_Z$ , in which case  $M_1^{\text{eff}} \simeq m_{\tilde{\chi}_1^0}$ ,  $M_2^{\text{eff}} \simeq m_{\tilde{\chi}_1^+}$ , and  $|\mu^{\text{eff}}| \simeq m_{\tilde{\chi}_3^0}$  hold, where  $M_1^{\text{eff}}$ ,  $M_2^{\text{eff}}$ , and  $-\mu^{\text{eff}}$  are the (1,1), (2,2), and (3,4) elements of the effective neutralino mass matrix  $\bar{Y}_{ij}$ , defined in Eq. (B.6).

	$\tilde{e}_L^- \tilde{e}_L^+$	$\tilde{e}_R^- \tilde{e}_R^+$	$\tilde{e}_L^- \tilde{e}_R^+$	$\tilde{e}_R^- \tilde{e}_L^+$	$\tilde{\nu}_e \tilde{\nu}_e^*$
$e_L^-$	105	8.83	121	0	678
$e_R^-$	8.83	235	0	121	9.81

Table 1: Total tree-level cross-sections, in fb, of  $e^-e^+ \rightarrow \tilde{\ell}_i \tilde{\ell}_j^*$  for the various modes. Input parameters are given in the text.

We show in Fig. 3 the  $M_{\tilde{Q}}$  dependence of the cross-sections for  $m_{\tilde{\chi}_1^0} = 100$  GeV,  $m_{\tilde{\chi}_1^+} = 200$  GeV,  $m_{\tilde{\chi}_3^0} = 300$  GeV,  $\tan\beta(M_Z) = 4$ ,  $m_{\tilde{\ell}} = 200$  GeV,  $A = 0$ ,  $\mu < 0$ , and  $\sqrt{s} = 500$  GeV. Here we normalize the cross-sections to the tree-level values. The tree-level cross-sections are functions of the standard model gauge couplings  $\hat{g}_i^{\text{eff}}(Q)$  (at  $Q = 200$  GeV) and the tree-level  $M_i$ ,  $\mu$  and  $\tan\beta$ . The latter parameters are found by inverting the tree-level relations between  $M_i$ ,  $\mu$ ,  $\tan\beta$  and the input masses  $m_{\tilde{\chi}_1^0}$ ,  $m_{\tilde{\chi}_1^+}$  and  $m_{\tilde{\chi}_3^0}$ . Hence, the tree-level cross-sections are independent of the squark mass scale. The numerical values of the tree-level cross-sections are listed in Table 1.

The one-loop corrected cross-sections of the modes which have a  $t$ -channel contribution are similar to tree-level ones at  $M_{\tilde{Q}} \lesssim 300$  GeV, but increase linearly with  $\log M_{\tilde{Q}}$ . Because the effective masses are equal to the input pole masses to  $\mathcal{O}((p^2 - m_{\tilde{\chi}}^2)/M_{\tilde{Q}}^2)$ , the squark mass dependence of the one-loop corrected cross-sections is primarily due to the difference between the effective theory gauge and gaugino couplings.

The two channels which have  $\tilde{W}$  contributions ( $e_L^- e^+ \rightarrow \tilde{e}_L^- \tilde{e}_L^+, \tilde{\nu}_e \tilde{\nu}_e^*$ ) show the largest  $M_{\tilde{Q}}$  dependence. The destructive interference between the  $s$ - and  $t$ -channel amplitudes accounts for the enhancement of the  $\tilde{e}_L^- \tilde{e}_L^+$  correction relative to the  $\tilde{\nu}_e \tilde{\nu}_e^*$  case. Other channels  $e_L^- e^+ \rightarrow \tilde{e}_L^- \tilde{e}_R^+, e_R^- e^+ \rightarrow \tilde{e}_R^- \tilde{e}_R^+, \tilde{e}_R^- \tilde{e}_L^+$  show smaller  $M_{\tilde{Q}}$  dependence from  $\tilde{B}$  contributions. Nevertheless, these  $M_{\tilde{Q}}$  dependences are significantly larger than the renormalization scale dependence of the corrected cross-sections (see Fig. 2). In contrast, the remaining channels, which have only  $s$ -channel contributions, show very little  $M_{\tilde{Q}}$  dependence, as explained in Section 2.

We now consider two approximations to the full calculation. First, we consider the effective theory approximation (ETA), where the effective masses, couplings, and mixing matrices are used in the  $t$ -channel amplitudes (see Eq. (8)). We make a further approximation in the ETA by fixing the momenta of the effective parameters to an average  $t$ -channel momentum,  $p^2 = -m_{\tilde{\ell}}^2$ . The second approximation is the leading log approximation (LLA), which is the ETA in leading logarithm approximation.

The full calculation differs from the ETA by  $\mathcal{O}(M_Z^2/M_{\tilde{Q}}^2)$  terms which arise when factorizing the amplitude (and by  $\mathcal{O}((p^2 + m_{\tilde{\ell}}^2)/M_{\tilde{Q}}^2)$  corrections due to fixing  $p^2$ ). The LLA differs additionally by constant and  $\mathcal{O}(1/M_{\tilde{Q}}^2)$  corrections. Figs. 4(a) and (b) shows the full correction, the ETA, and the LLA, for  $\sigma(e^-e^+ \rightarrow \tilde{e}_R^- \tilde{e}_R^+)$  and  $\sigma(e^-e^+ \rightarrow \tilde{\nu}_e \tilde{\nu}_e^*)$ , respectively. In Fig. 4(b) we use the effective coupling  $\bar{g}_{e\tilde{e}_L\tilde{W}}(-m_{\tilde{\ell}}^2)$ , rather than  $\bar{g}_{e\tilde{\nu}_e\tilde{W}}(-m_{\tilde{\ell}}^2)$ , which introduces additional  $\mathcal{O}((M_Z^2, m_t^2)/M_{\tilde{Q}}^2)$  differences between the full and ETA calculations. Figs. 4 show that the full calculation is well approximated by the ETA, even for small squark masses. The LLA does correctly describe the logarithmic increase in the full correction (as the name implies), but there is a constant difference

of 0.6% [1.0%] seen between the full and LLA curves in Fig. 4(a) [(b)]. This constant difference is largely accounted for by the correct matching of the effective coupling, where, at zero momentum, and for zero quark mass, the logarithms in Eq. (1) are replaced as [9]

$$\ln\left(\frac{M_{\tilde{Q}}}{m_{\tilde{\ell}}}\right) \quad \longrightarrow \quad \ln\left(\frac{M_{\tilde{Q}}}{m_{\tilde{\ell}}}\right) - 3/8 .$$

In Fig. 4 there is a slight discrepancy between the ETA and the full results at very large  $M_{\tilde{Q}}$ . This is due to the resummation of the effective mass corrections inherent in the derivation of the effective amplitude.

Before leaving this section, we comment on the dependence of the cross-sections on the parameter  $A = A_t/M_{\tilde{Q}} = A_b/M_{\tilde{Q}}$ , which can give sub-leading corrections through the left-right mixing of third generation squarks. One might expect that the  $A$  dependence could become significant for small ( $\sim 1$ ) values of  $\tan\beta$ . Fig. 5 shows that for  $\tan\beta(M_Z) = 1.5$  the dependence is much smaller than the  $M_{\tilde{Q}}$  dependence. For the case  $\mu < 0$ , the cross-section is almost independent of  $A$  if  $M_{\tilde{Q}} \gtrsim 1$  TeV. For  $\mu > 0$ , there is more dependence. For example, for  $M_{\tilde{Q}} = 1$  TeV, the cross-section increases by about 3 per cent as  $A$  varies from  $-3$  to  $+3$ .

## 4 $\Delta\chi^2$ analysis

In the previous section, we have shown the squark mass dependence of the slepton production cross-section  $\sigma^{\text{one-loop}}(e^-e^+ \rightarrow \tilde{\ell}\tilde{\ell}^*)$ . We found the cross-sections are well described by that of an effective theory, where the tree-level relations between the fermion-sfermion-gaugino couplings and the gauge couplings are renormalized. In this section, we consider the determination of the squark mass  $M_{\tilde{Q}}$  through the measurement of the slepton production cross-section.

As described in section 2, the sfermion and chargino/neutralino production cross-sections depend on the gaugino mass parameters  $M_1$  and  $M_2$ , the Higgsino mass parameter  $\mu$ , the ratio of the vacuum expectation values  $\tan\beta$ , and the sfermion mass  $m_{\tilde{\ell}}$ . The cross-sections also depend on the effective fermion-sfermion-gaugino coupling  $\bar{g}_{f\tilde{f}\tilde{\chi}}$ , which is nicely parameterized by  $\log M_{\tilde{Q}}$ . By constraining  $\bar{g}_{f\tilde{f}\tilde{\chi}}$  we can determine  $M_{\tilde{Q}}$ , if the rest of the parameters are known accurately enough.

It has been demonstrated that an accurate determination of  $m_{\tilde{\chi}}$  and  $m_{\tilde{\ell}}$  is indeed possible if sfermions  $\tilde{\ell}$  are produced and dominantly decay into a charged lepton  $\ell'$  and a chargino or neutralino  $\tilde{\chi}$ . The simple kinematics of the two body decays result in a flat energy distribution of the final state leptons between the endpoint energies  $E_{\text{min}}^{\ell'}$  and  $E_{\text{max}}^{\ell'}$ , which are simple functions of  $\sqrt{s}$ ,  $m_{\tilde{\ell}}$ , and  $m_{\tilde{\chi}}$ . The measured endpoint energies therefore determine  $m_{\tilde{\ell}}$  and  $m_{\tilde{\chi}}$ .

In Ref. [4], the results of detailed MC simulations were presented for  $\tilde{\mu} \rightarrow \mu\tilde{\chi}_1^0$  and  $\tilde{e} \rightarrow e\tilde{\chi}_1^0$ . It was shown that the  $\tilde{\ell}_R$  and  $\tilde{\chi}_1^0$  masses could be measured to better than 1%. Recently, Baer et al. [7] performed a MC study for the case that left-handed sfermions are produced and decay into a gaugino-like chargino or neutralinos. In their example called point 3,  $\tilde{\nu}_e\tilde{\nu}_e^*$  production is followed by  $\tilde{\nu}_e^{(*)} \rightarrow e^\mp\tilde{\chi}_1^\pm$ . The decay mode  $\tilde{\nu}_e\tilde{\nu}_e^* \rightarrow e^-e^+\tilde{\chi}_1^+\tilde{\chi}_1^- \rightarrow e^-e^+\mu 2j$  ( $\nu_\mu 2\tilde{\chi}_1^0$ ) is background free and the measured electron endpoint energies allow for a 1% measurement of  $m_{\tilde{\chi}_1^\pm}$  and  $m_{\tilde{\nu}}^2$ .

---

<sup>2</sup>Notice that the mass errors are considerably improved over those obtained from the  $e^+e^- \rightarrow \tilde{\chi}_1^+\tilde{\chi}_1^-$  process [4].



The results of Ref. [7] encourage us to consider their example point 3. The chosen parameter set corresponds to  $m_{\tilde{\nu}_e} = 207$  GeV,  $m_{\tilde{\chi}_1^+} = 96$  GeV,  $m_{\tilde{\chi}_1^0} = 45$  GeV and  $m_{\tilde{\chi}_3^0} = 270$  GeV, and the lightest chargino and neutralinos are gaugino-like. Their study suggests that we can take  $m_{\tilde{\chi}_1^+}$ ,  $m_{\tilde{\chi}_1^0}$ , and  $m_{\tilde{\nu}_e}$  as well constrained input parameters. For  $20 \text{ fb}^{-1}$  of luminosity, their MC simulations show that at 68% CL,  $(\delta m_{\tilde{\chi}_1^+}, \delta m_{\tilde{\nu}_e}) = (1.5 \text{ GeV}, 2.5 \text{ GeV})$ .

In the following we estimate the statistical significance of the radiative correction to the production cross-section. To most effectively constrain the squark mass we would take into account all the possible channels. However, for the purposes of this paper, it suffices for us to focus solely on the  $\tilde{\nu}_e$  production cross-section, because it is larger than 1 pb for a left-handed electron beam, and larger than the other sparticle production cross-sections at  $\sqrt{s} = 500$  GeV.

The sensitivity of the sneutrino production cross-section on the chargino mixing is determined by the sign of  $\mu$ . For  $\mu < 0$ , the gaugino/Higgsino mixing is suppressed, and hence the cross-section depends mildly on  $\tan\beta$ . Also, there is very little  $m_{\tilde{\chi}_3^0}$  dependence in this case. For  $\mu > 0$ , the mixing gives rise to significant  $\tan\beta$  and  $m_{\tilde{\chi}_3^0}$  dependence. The heavy chargino and neutralinos are produced once  $\sqrt{s} > 2|\mu|$ , and we assume that these masses can be constrained to a reasonable range<sup>3</sup>. Also, if  $\mu$  is not too large, the splitting of the heavy chargino and neutralino masses is quite different for the different signs of  $\mu$ . If the splitting can be measured, the sign of  $\mu$  might be determined. For example, at point 3 with  $m_{\tilde{\chi}_3^0} = 270$  GeV and  $\mu < 0$  ( $\mu > 0$ ),  $m_{\tilde{\chi}_4^0} - m_{\tilde{\chi}_3^0} = 5$  (27) GeV. The reasonably large production cross-sections of the heavier chargino and neutralinos ( $\mathcal{O}(100)$  fb at  $\sqrt{s} = 800$  GeV) give us hope that these mass differences can be distinguished. As long as  $m_{\tilde{\chi}_3^0}$  is known to  $\mathcal{O}(5\text{-}10\%)$  and the sign of  $\mu$  can be determined, the chargino mixing uncertainty will not significantly affect the determination of the effective coupling  $\bar{g}_{e\tilde{\nu}_e\tilde{W}}$ .

We would first like to provide a feel for the sensitivity to the squark mass scale and  $\tan\beta$  in the ideal case where we ignore the slepton and gaugino mass uncertainties. In Fig. 6 we show the statistical significance of the loop correction by plotting contours of constant cross-section. Here we fix the sneutrino mass and determine  $\mu$ ,  $M_1$  and  $M_2$  by fixing the one-loop corrected masses  $m_{\tilde{\chi}_1^0}$ ,  $m_{\tilde{\chi}_3^0}$ , and  $m_{\tilde{\chi}_1^+}$ . Rather than plot the contours according to the value of the production cross-section, we plot the contours corresponding to the number of standard deviations of the fluctuation of the accepted number of events. The  $1\text{-}\sigma$  fluctuation corresponds to  $\sqrt{N_{\text{input}}}$ , where  $N_{\text{input}}$  is our nominal value of the number of events at  $M_{\tilde{Q}} = 1000$  GeV and  $\tan\beta(M_Z) = 4$ . The accepted number of events  $N$  is given by

$$N = A \cdot \sigma(e_L^- e^+ \rightarrow \tilde{\nu}_e \tilde{\nu}_e) \times \left( \text{BR}(\tilde{\nu}_e \rightarrow e \tilde{\chi}_1^+) \right)^2 \times 100 \text{ fb}^{-1}. \quad (12)$$

Here we took  $\text{BR}(\tilde{\nu}_e \rightarrow e \tilde{\chi}_1^+) = 0.6$  and overall acceptance  $A = 0.28$ <sup>4</sup>. The number of accepted events at our nominal point  $N_{\text{input}}$  is about 12800 for  $\mu < 0$  and 11900 for  $\mu > 0$ .

The mass measurement from the jet energy distributions in chargino decay  $\tilde{\chi}_1^+ \rightarrow \tilde{\chi}_1^0 q \bar{q}$  gives only a few percent measurement of the masses due to the uncertainty in the jet momentum.

<sup>3</sup>The heavier chargino and neutralinos dominantly decay to a  $W$  or  $Z$  and a wino-like neutralino or chargino (through its suppressed Higgsino component). The dominant decay process gives maximally 8 jets in the final state, and the background to the process is small. If the energy distribution of the gauge bosons in these decays could be measured, the endpoint technique could also be applied here.

<sup>4</sup>The acceptance given in Ref. [4] is 45% for  $m_{\tilde{e}_R} = 142$  GeV,  $m_{\tilde{\chi}_1^0} = 118$  GeV and  $\sqrt{s} = 350$  GeV. We further scale our acceptance down, because our calculation of cross-section does not include the effects of initial state radiation, beam energy spread, and beamstrahlung.

We show the contours for  $\mu < 0$  in Fig. 6(a). If  $\tan\beta$  is well measured,  $M_{\tilde{Q}}$  is constrained to  $M_{\tilde{Q}} = 1000_{-280}^{+370}$  GeV at 1- $\sigma$  significance. If instead we assume the constraint  $2 < \tan\beta < 8$ , the mild  $\tan\beta$  dependence yields  $700 < M_{\tilde{Q}} < 1900$  GeV. In the case  $\mu > 0$  (Fig. 6(b)), increasing the squark mass can be compensated for by decreasing  $\tan\beta$ , and measuring sneutrino production then determines a region of the  $(M_{\tilde{Q}}, \tan\beta)$  plane. As with  $\mu < 0$ ,  $M_{\tilde{Q}}$  is decently constrained if  $\tan\beta$  is known ( $M_{\tilde{Q}} = 1000_{-450}^{+350}$  GeV). However, if we have  $2 < \tan\beta < 8$ , only the uninteresting bound  $M_{\tilde{Q}} < 10$  TeV can be achieved.

In Fig. 6(c) we show the contours again for  $\mu > 0$ , but now we raise  $m_{\tilde{\chi}_3^0}$  to 500 GeV. Larger values of  $\mu$  lead to weaker  $\tan\beta$  dependence. However, in this case the cross-section is still sensitive to the heavy chargino mass  $m_{\tilde{\chi}_2^+}$ . If the heavier chargino is beyond the kinematical reach of the collider, there may be considerable uncertainty in the predicted cross-section. The cross-section is pretty much independent of  $\mu$  once  $\mu > 850$  GeV, in this case. If we vary  $\mu$  from 450 to 850 GeV the cross-section varies by about 2%. It is good to keep in mind that  $\mu$  may be constrained in a situation such as this by measuring the left-right asymmetry of the lighter chargino production cross-section.

Figs. 6 illustrate that we might have to rely on independent measurements of  $\tan\beta$  in order to obtain a nice constraint on  $M_{\tilde{Q}}$ . For many regions in parameter space we expect  $\tan\beta$  will indeed be known fairly well. For example, it was pointed out by Ref. [5] that the measurement of the chargino forward-backward asymmetry provides a strong constraint on  $\tan\beta$  if  $M_2 \sim |\mu|$ . Also, for not too large slepton masses and  $\tan\beta \sim 1$ , the measurement of the mass difference between  $\tilde{e}_L$  and  $\tilde{\nu}_e$  gives a sensitive measurement of  $\tan\beta$ . Other measurements can be instrumental in pinning down  $\tan\beta$ . For example, the Higgs sector constraints on  $\tan\beta$  are considered in Ref. [20], which tend to give decent bounds for  $\tan\beta < 10$ .

We now turn to the effect of the mass uncertainties. The sneutrino production cross-section depends on the masses  $m_{\tilde{\nu}_e}$ ,  $m_{\tilde{\chi}_1^0}$ ,  $m_{\tilde{\chi}_3^0}$  and  $m_{\tilde{\chi}_1^+}$ . The uncertainties in these masses will of course worsen our ability to constrain the squark mass scale. Of these masses the cross-section is most sensitive to the sneutrino mass. All of the same chirality scalar production cross-sections suffer from the strong  $\beta_{\tilde{\ell}}^3$  kinematic dependence ( $\beta_{\tilde{\ell}} = \sqrt{1 - (m_{\tilde{\ell}}/E_{\text{beam}})^2}$ )<sup>5</sup>. Near threshold this results in an especially large sensitivity to the final-state mass. For example, a 1% uncertainty of  $m_{\tilde{\ell}}$  results in  $\delta\beta_{\tilde{\ell}}/\beta_{\tilde{\ell}} = 1.8\%$ , for  $m_{\tilde{\ell}} = 200$  GeV, and  $\sqrt{s} = 500$  GeV. This immediately translates into a 5.3% error in the total cross-section. Although a simple statistical scale-up of the results of Ref. [7] implies a sneutrino mass uncertainty of only 0.3%, this nevertheless leads to a significant degradation in our ability to constrain the squark mass scale. (Systematic errors might be the limiting factor here.)

Note, however, that the measurement of the sneutrino mass in Ref. [7] was obtained by studying a small fraction of the total sneutrino decay modes. The mode they studied,  $e^-e^+ \rightarrow \tilde{\nu}_e\tilde{\nu}_e^* \rightarrow e^-e^+\mu 2j(\nu_\mu 2\tilde{\chi}_1^0)$ , amounts to only about 4% of the total sneutrino decays. Using other modes, such as  $e^-e^+4j(2\tilde{\chi}_1^0)$ , might reduce the mass error even further. Because the  $\tilde{\nu}_e$  production cross-section is significantly larger than the other slepton cross-sections, isolating the various sneutrino signatures is less affected by SUSY backgrounds such as  $e^-e^+ \rightarrow \tilde{e}_L\tilde{e}_L^+ \rightarrow e^-e^+4j(2\tilde{\chi}_1^0)$ . In this discussion we assume the errors are dominantly statistical.

<sup>5</sup>The production cross-section  $\sigma(e^-e^+ \rightarrow \tilde{e}_R\tilde{e}_L)$  is proportional to  $\beta_{\tilde{\ell}}$ , due to the chiral structure of  $\ell\text{-}\tilde{\ell}_{L(R)}\text{-}\tilde{\chi}_i^0$  coupling.

Now we show the constraint on the squark mass  $M_{\tilde{Q}}$  after taking into account the uncertainty of the masses  $\delta m_{\tilde{\nu}_e}$  and  $\delta m_{\tilde{\chi}_1^+}$ . For this purpose, we define a  $\Delta\chi^2$  function as

$$\begin{aligned} \Delta\chi^2 &= \frac{\left(N(m_{\tilde{\chi}_1^0}, m_{\tilde{\chi}_3^0}, m_{\tilde{\chi}_1^+}, \tan\beta, m_{\tilde{\nu}_e}, M_{\tilde{Q}}) - N_{\text{input}}\right)^2}{N_{\text{input}}} \\ &+ \frac{(m_{\tilde{\chi}_1^+} - m_{\tilde{\chi}_1^+ \text{ input}})^2}{(\delta m_{\tilde{\chi}_1^+})^2} + \frac{(m_{\tilde{\nu}_e} - m_{\tilde{\nu}_e \text{ input}})^2}{(\delta m_{\tilde{\nu}_e})^2}. \end{aligned} \quad (13)$$

Here we consider the  $\mu < 0$  case, in which the  $\tilde{\chi}_1^0$  and  $\tilde{\chi}_3^0$  mass dependencies are negligible. We also assume that  $\tan\beta$  is well measured. In Fig. 7 we plot  $\Delta\chi_{\text{min}}^2$  against  $M_{\tilde{Q}}$ , where  $\Delta\chi_{\text{min}}^2$  is a minimum of  $\Delta\chi^2$  with respect to variations in  $m_{\tilde{\chi}_1^+}$  and  $m_{\tilde{\nu}_e}$ . By construction, the region of  $M_{\tilde{Q}}$  where  $\sqrt{\Delta\chi_{\text{min}}^2} < 1, 2, \dots$  corresponds to 1, 2,  $\dots$ - $\sigma$  error of the squark mass when the chargino and sneutrino mass uncertainties are taken into account. The sneutrino mass uncertainty reduces the sensitivity of the production cross-section to  $M_{\tilde{Q}}$  considerably, because the effect of increasing  $M_{\tilde{Q}}$  can be compensated for by a small increase in  $m_{\tilde{\nu}_e}$ . On the other hand, we do not find any significant effect due to non-zero  $\delta m_{\tilde{\chi}_1^+}$ .

From Fig. 7 we see that in this case, even with the sneutrino mass uncertainty, we can reasonably constrain the squark mass scale. For example, at the 1- $\sigma$  level with  $M_{\tilde{Q}} = 1$  TeV, we constrain  $M_{\tilde{Q}}$  to  $1_{-0.5}^{+1.2}$  TeV, using the naive scale up (from 20 fb $^{-1}$  to 100 fb $^{-1}$ ) of the statistical errors of Ref. [7]. This corresponds to the difference between the gauge and gaugino effective couplings,  $\delta g_2/g_2 = 0.011 \pm 0.006$ . This can be compared to the estimate of the constraint  $\delta g_2/g_2 = \pm 0.02$  from the chargino production measurement [10]. Such comparisons are sensitive to different choices of parameter space and other assumptions. The sensitivity of the constraint on the mass errors can be seen by changing the errors. If we reduce the mass uncertainties by a factor of 2, we find the interesting constraint  $600 < M_{\tilde{Q}} < 1500$  GeV.

Fig. 7 illustrates the large dependence on the mass uncertainties. This sensitivity is greatly reduced in the case of chargino production. As we mentioned previously, the  $t$ -channel amplitude is very similar to that of sneutrino production; only its final and intermediate states are exchanged. The external chargino wave-function renormalization induces the same  $\log M_{\tilde{Q}}$  correction to the  $e\text{-}\tilde{\nu}_e\text{-}\tilde{\chi}_1^+$  coupling. Also, the chargino production cross-section is generally large; for the set of parameters considered, it is near 1 pb for a left-handed electron beam. Because the chargino cross-section is only proportional to a single power of  $\beta$ , the uncertainty in the cross-section due to the final state mass is effectively reduced by a factor of 3. Notice  $m_{\tilde{\chi}_1^+}$  can be measured through the electron energy distribution from the  $\tilde{\nu}_e$  production and decay. Also, the chargino production cross-section rises quickly near threshold, which allows for a determination of its mass by a threshold scan.

In Figs. 6 and 7, we assumed that the decays into the lightest chargino  $\tilde{\chi}_1^\pm$  were detectable as  $\tilde{\nu}_e$  production signal without background. This may not be true, depending on the decay mode of the chargino. For example, if both of the charginos decay into  $q\bar{q}'\tilde{\chi}_1^0$ , it gives an  $e^-e^+4j$  signal event with missing energy. Pair production of  $\tilde{e}_L\tilde{e}_L$  could give the same  $e^-e^+4j$  signal with similar kinematics. By SU(2) invariance  $\tilde{e}_L$  and  $\tilde{\nu}_e$  are very close in mass, so it is natural to think that this background is necessarily problematic. Additionally, at point 3 Ref. [7] estimates that the  $\tilde{e}_L$

mass uncertainty is larger than that of  $\tilde{\nu}_e$ ; this corresponds to a large uncertainty in the expected  $\tilde{e}_L$  production cross-section. Fortunately, in this case, the cross-section of  $\tilde{e}_L$  and its branching ratio into  $\tilde{\chi}_2^0$  are small, and they are constrained by other measurements, so they give a negligible background to the  $\tilde{\nu}_e\tilde{\nu}_e^* \rightarrow e^-e^+4j$  signal.

We also assumed constant  $\text{BR}(\tilde{\nu}_e \rightarrow e\tilde{\chi}_1^+)$  throughout Figs. 6 and 7, while the branching ratio is expected to vary with  $M_2$ ,  $\mu$ ,  $\tan\beta$ ,  $m_{\tilde{t}}$ , and  $M_{\tilde{Q}}$ . Notice,  $M_2$ ,  $\mu$ , and  $m_{\tilde{t}}$  are constrained from mass measurements, while in Fig. 6  $\tan\beta$  and  $M_{\tilde{Q}}$  are our fit parameters, so the inclusion of the branching ratio would not introduce additional uncertainty in the  $M_{\tilde{Q}}$  constraint unless there is a large correlation. The chargino branching ratios ( $B(\tilde{\chi}^+ \rightarrow jj\tilde{\chi}^0)$  and  $B(\tilde{\chi}^+ \rightarrow \ell\nu\tilde{\chi}^0)$ ) are likewise determined by the measured sparticle masses and their cross-section and fit parameters, or they are directly constrained by the study of chargino and neutralino production at low energy<sup>6</sup>.

We did not include the expected luminosity and acceptance errors. Needless to say, it is extremely important to achieve a low luminosity error, since we are dealing with a potentially sub-percent measurement. The effect of the luminosity error can be directly seen in Fig. 6. In the chargino study of Ref. [5], the systematic error of acceptance is claimed to be significant in the two jet + lepton final state. There, the large background from  $WW$  production requires a very tight cut, leading to low acceptance and large systematic error. Here, we consider sneutrino production followed by decays to charginos. There is very low SM background to the final state  $e^+e^- + (4j \text{ or } 2j\ell \text{ or } \ell\ell') + \text{missing energy}$ , where the final state electron and positron are hard and isolated. Also, the SM background has very different kinematical structure from the signal. Given the precisely measured chargino, neutralino and sneutrino masses, it is reasonable to assume the acceptance error is negligible.

In Ref. [5], the possibility to measure  $g_{e\tilde{\nu}_e\tilde{W}}$  from chargino production has been studied, resulting in a rather poor constraint ( $\mathcal{O}(20\%)$ ). In that analysis, the assumption was made that only chargino production was accessible. This leads to a rather large uncertainty due to the unknown sneutrino mass, which could only be determined with a polarized beam through the differential cross-section of the chargino production itself. That was a reasonable and conservative assumption at the time, before a detailed MC simulation of  $\tilde{\nu}_e$  production was available. Including the sneutrino mass measurement will in this case provide a reasonable constraint on  $\bar{g}$  and hence on the squark mass [10]; a detailed study will be presented elsewhere [21].

## 5 Conclusions

Supersymmetry is a beautiful symmetry which relates bosons and fermions. If we wish to determine whether this symmetry is realized in nature, the relations imposed between particles and their superpartners must be confirmed by experiment. Of course, discovering a particle with the quantum numbers of a superpartner is the first very important step in this procedure. An equally important test, though, is the confirmation of the hard relations imposed by supersymmetry, for example, the equivalence of the gauge and gaugino couplings.

It has been argued that a next generation linear collider would be an excellent tool to verify

---

<sup>6</sup>When the chargino cannot decay to an on-shell  $W$ -boson, the branching ratios become somewhat sensitive to squark and slepton masses.

supersymmetry in this respect. Production cross-sections such as  $\sigma(e^-e^+ \rightarrow \tilde{\ell}\tilde{\ell}^*)$  and  $\sigma(e^-e^+ \rightarrow \tilde{\chi}_i^- \tilde{\chi}_i^+)$  involve the  $t$ -channel exchange of gauginos or sleptons, so they depend on gaugino couplings. Several papers [8, 5] have shown that it is possible to verify the equivalence of the gaugino and gauge couplings in a model independent way, by fitting the data to the cross-sections with arbitrary gaugino couplings. The sensitivity ranges from about 1% to 10%, depending on the assumptions.

In this paper, we approached this problem from a somewhat different direction. Because supersymmetry must be badly broken by soft breaking terms, the tree-level relations of the couplings are also broken, by radiative corrections. The corrections are logarithmically sensitive to the splitting of the supersymmetry multiplets. To quantify this, we have calculated the full one-loop correction due to (s)quark loops of the slepton production cross-sections. We have explicitly demonstrated that the full one-loop amplitudes can be factorized into a form which corresponds to an effective theory in which the heavy squarks are integrated out. The difference between the effective lepton-slepton-gaugino couplings  $\bar{g}_{\ell\tilde{\ell}\tilde{\chi}_i}$  and the effective gauge couplings  $\hat{g}_i^{\text{eff}}$  is given by a coupling factor times  $\log M_{\tilde{Q}}/m_{\tilde{\ell}}$ . The one-loop formulae for the chargino and neutralino production cross-sections are not given in this paper, but the effective gaugino couplings receive the same corrections to logarithmic accuracy.

We gave an explicit example which illustrates that the statistics at the future linear collider may be enough to constrain the squark mass scale through the measurement of the slepton production cross-section. We found, with 1- $\sigma$  significance,  $M_{\tilde{Q}}$  could be constrained to  $1_{-0.5}^{+1.2}$  TeV by the measurement of the sneutrino production cross-section. This corresponds to a measurement of the difference between the SU(2) gauge and gaugino couplings  $\delta g_2/g_2 = 0.011 \pm 0.006$ . We found this constraint in the  $\mu < 0$  case where we took into account the errors (based on existing MC simulation) of the sneutrino and light chargino masses, but assumed  $\tan\beta$  was well constrained by other measurements. In the  $\mu > 0$  case the slepton cross-sections are much more sensitive to  $\tan\beta$  and the heavy (Higgsino dominated) chargino and neutralino masses. We need to rely on additional measurements in order to precisely measure the gaugino couplings in this case.

For either sign of  $\mu$ , the mass of the sleptons and gauginos must be measured very precisely in order to successfully constrain the squark mass scale via production cross-section measurements. The effect of the slepton mass uncertainty on the prediction of the slepton production cross-section is especially significant, as discussed in Section 4. In order to determine the ultimate sensitivity of this procedure, a thorough study of the systematic uncertainties in the slepton mass measurements is necessary. The prediction of the chargino production cross-section is less sensitive to the uncertainties in the masses. The limiting factor in the chargino mode is SM background and statistics.

It is important to note that the constraint on the squark mass scale can be stronger than the one presented in this paper. Here, we estimated the sensitivity to squark mass scale by utilizing sneutrino production followed by its decay into a chargino and an electron. Depending on the spectrum and center-of-mass energy, there will typically be many other production processes which involve  $t$ -channel exchange of gauginos or sleptons, and all those amplitudes have  $\log M_{\tilde{Q}}$  corrections.

The constraint on the squark mass we have realized here could be unique in the sense that this information may not be available at the LHC. Even if the LHC squark production rate is large, the gluino could be produced in even larger numbers, creating a large irreducible background to

the squark signal. A large gluino background could make the extraction of the squark mass from kinematical variables difficult.

On the other hand, if information on the squark masses is obtained at the LHC, we would have rather accurate predictions for the gaugino couplings. In this case, the measurement of the production cross-sections we considered here would constrain new supersymmetry-breaking physics with standard model gauge quantum numbers. In a sense, the study proposed here is similar in nature to studies performed at LEP and SLC. The physics of gauge boson two-point functions has been studied extensively at LEP and SLC, and it has provided strong constraints on new physics. Similarly, a future LC and the LHC might provide precision studies of the gaugino two-point functions, to realize a supersymmetric version of new precision tests.

## Acknowledgements

We thank Manuel Drees and Jonathan Feng for useful discussions.

## Appendix A: One-loop quark/squark corrections

In this section, we show the explicit forms of the quark-squark loop corrections to the amplitudes of the processes  $e^-(p_1)e^+(p_2) \rightarrow \tilde{\ell}_i(p_3)\tilde{\ell}_j^*(p_4)$  where  $\tilde{\ell}_i = (\tilde{e}_L^-, \tilde{e}_R^-, \tilde{\nu}_e)$ . We adopt the  $\overline{\text{DR}}$  renormalization scheme, and the  $\overline{\text{DR}}$  suffix is implicit throughout this and the next sections.

The neutralino  $\overline{\text{DR}}$  mass matrix  $Y_N$  and the chargino mass matrix  $Y_C$  are functions of  $M_1(Q)$ ,  $M_2(Q)$ ,  $\mu(Q)$ ,  $\tan\beta(Q)$ ,  $M_W(Q)$ , and  $M_Z(Q)$  as follows [19],

$$Y_N(Q)(\tilde{B}, \tilde{W}^3, \tilde{H}_1^0, \tilde{H}_2^0) \equiv \begin{pmatrix} M_1 & 0 & -M_Z c_\beta s_W & M_Z s_\beta s_W \\ 0 & M_2 & M_Z c_\beta c_W & -M_Z s_\beta c_W \\ -M_Z c_\beta s_W & M_Z c_\beta c_W & 0 & -\mu \\ M_Z s_\beta s_W & -M_Z s_\beta c_W & -\mu & 0 \end{pmatrix}. \quad (\text{A.1})$$

Here  $c_\beta \equiv \cos\beta$ ,  $s_\beta \equiv \sin\beta$ ,  $c_W \equiv M_W/M_Z$  and  $s_W \equiv \sqrt{1 - c_W^2}$ . The  $Q$  dependence of the right hand side is implicit. A unitary matrix  $N$  is defined so that  $M_N^D = (m_{\tilde{\chi}_i^0} \delta_{ij}) = N^* Y_N N^\dagger$ . The chargino  $\overline{\text{DR}}$  mass matrix is

$$Y_C(Q)(\tilde{W}, \tilde{H}) \equiv \begin{pmatrix} M_2 & \sqrt{2}M_W s_\beta \\ \sqrt{2}M_W c_\beta & \mu \end{pmatrix}, \quad (\text{A.2})$$

and the chargino mass matrix can be diagonalized by two unitary matrices  $U$  and  $V$  as  $M_C^D \equiv U^* Y_C V^\dagger$ . We order the charginos and neutralinos according to their masses, so, for example,  $\tilde{\chi}_1^0$  is the lightest neutralino.

We first show the  $t$ -channel amplitudes. They are expressed in terms of two-point functions  $iK_{0ij}$ ,  $iK_{-ij}$  of neutralinos  $\tilde{\chi}_i^0 \tilde{\chi}_j^0$  and charginos  $\tilde{\chi}_i^+ \tilde{\chi}_j^-$ .  $K_{ij}$  are decomposed as

$$K_{ij} = \Sigma_{ij}^L(p^2) \not{p} P_L + \Sigma_{ij}^R(p^2) \not{p} P_R + \Sigma_{ij}^M(p^2) P_L + \Sigma_{ij}^{M*}(p^2) P_R, \quad (\text{A.3})$$

where the momentum  $p$  flows from  $j$  to  $i$ .  $P_{R,L}$  are the chiral projectors,  $(1 \pm \gamma_5)/2$ .

In the following the argument of the  $\Sigma$  functions is  $p^2$ . The corrected  $t$ -channel amplitude  $i\mathcal{M}_{LL}^{(t)}$  for  $\tilde{e}_L^- \tilde{e}_L^+$  is then expressed as

$$i\mathcal{M}_{LL}^{(t)} = -i\bar{v}(p_2)\not{p}P_L u(p_1)a_{\tilde{e}_L i}^{0*}a_{\tilde{e}_L j}^0 \left[ \frac{\delta_{ij}}{p^2 - m_{\tilde{\chi}_i^0}^2} - \frac{1}{(p^2 - m_{\tilde{\chi}_i^0}^2)(p^2 - m_{\tilde{\chi}_j^0}^2)} \left( m_{\tilde{\chi}_i^0} m_{\tilde{\chi}_j^0} \Sigma_{0ij}^L + p^2 \Sigma_{0ij}^R + m_{\tilde{\chi}_j^0} \Sigma_{0ij}^M + m_{\tilde{\chi}_i^0} \Sigma_{0ij}^{M*} \right) \right], \quad (\text{A.4})$$

where  $p = p_1 - p_3 = p_4 - p_2$ . Similarly, other  $t$ -channel amplitudes are

$$i\mathcal{M}_{RR}^{(t)} = -i\bar{v}(p_2)\not{p}P_R u(p_1)b_{\tilde{e}_R i}^{0*}b_{\tilde{e}_R j}^0 \left[ \frac{\delta_{ij}}{p^2 - m_{\tilde{\chi}_i^0}^2} - \frac{1}{(p^2 - m_{\tilde{\chi}_i^0}^2)(p^2 - m_{\tilde{\chi}_j^0}^2)} \left( p^2 \Sigma_{0ij}^L + m_{\tilde{\chi}_i^0} m_{\tilde{\chi}_j^0} \Sigma_{0ij}^R + m_{\tilde{\chi}_i^0} \Sigma_{0ij}^M + m_{\tilde{\chi}_j^0} \Sigma_{0ij}^{M*} \right) \right], \quad (\text{A.5})$$

$$i\mathcal{M}_{LR}^{(t)} = -i\bar{v}(p_2)P_L u(p_1)b_{\tilde{e}_R i}^{0*}a_{\tilde{e}_L j}^0 \left[ \frac{m_{\tilde{\chi}_i^0} \delta_{ij}}{p^2 - m_{\tilde{\chi}_i^0}^2} - \frac{1}{(p^2 - m_{\tilde{\chi}_i^0}^2)(p^2 - m_{\tilde{\chi}_j^0}^2)} \left( p^2 (m_{\tilde{\chi}_j^0} \Sigma_{0ij}^L + m_{\tilde{\chi}_i^0} \Sigma_{0ij}^R) + m_{\tilde{\chi}_i^0} m_{\tilde{\chi}_j^0} \Sigma_{0ij}^M + p^2 \Sigma_{0ij}^{M*} \right) \right], \quad (\text{A.6})$$

$$i\mathcal{M}_{RL}^{(t)} = -i\bar{v}(p_2)P_R u(p_1)a_{\tilde{e}_L i}^{0*}b_{\tilde{e}_R j}^0 \left[ \frac{m_{\tilde{\chi}_i^0} \delta_{ij}}{p^2 - m_{\tilde{\chi}_i^0}^2} - \frac{1}{(p^2 - m_{\tilde{\chi}_i^0}^2)(p^2 - m_{\tilde{\chi}_j^0}^2)} \left( p^2 (m_{\tilde{\chi}_i^0} \Sigma_{0ij}^L + m_{\tilde{\chi}_j^0} \Sigma_{0ij}^R) + p^2 \Sigma_{0ij}^M + m_{\tilde{\chi}_i^0} m_{\tilde{\chi}_j^0} \Sigma_{0ij}^{M*} \right) \right], \quad (\text{A.7})$$

$$i\mathcal{M}_{\nu\nu}^{(t)} = -i\bar{v}(p_2)\not{p}P_L u(p_1)a_{\tilde{\nu}_L i}^{-*}a_{\tilde{\nu}_L j}^- \left[ \frac{\delta_{ij}}{p^2 - m_{\tilde{\chi}_i^+}^2} - \frac{1}{(p^2 - m_{\tilde{\chi}_i^+}^2)(p^2 - m_{\tilde{\chi}_j^+}^2)} \left( m_{\tilde{\chi}_i^+} m_{\tilde{\chi}_j^+} \Sigma_{-ij}^L + p^2 \Sigma_{-ij}^R + m_{\tilde{\chi}_j^+} \Sigma_{-ij}^M + m_{\tilde{\chi}_i^+} \Sigma_{-ij}^{M*} \right) \right], \quad (\text{A.8})$$

Here  $(a, b)$  denote the couplings of neutralinos and charginos to fermions and sfermions,

$$\begin{aligned} \mathcal{L}_{\text{int}} = & -\tilde{f}_i^* \tilde{\chi}_j^0 (a_{\tilde{f}ij}^0 P_L + b_{\tilde{f}ij}^0 P_R) f + (\text{h.c.}) \\ & -\tilde{f}_{1i}^* \tilde{\chi}_j^- (a_{\tilde{f}1ij}^- P_L + b_{\tilde{f}1ij}^- P_R) f_2 + (\text{h.c.}) \\ & -\tilde{f}_{2i}^* \tilde{\chi}_j^+ (a_{\tilde{f}2ij}^+ P_L + b_{\tilde{f}2ij}^+ P_R) f_1 + (\text{h.c.}), \end{aligned} \quad (\text{A.9})$$

where  $f = (q, l)$  and  $(f_1, f_2)$  are SU(2) doublets. Explicit forms of  $(a, b)$  for the gauge eigenstates of  $\tilde{f}$  are written in terms of mixing matrices  $(N, U, V)$  and Yukawa couplings  $y_f$  of fermions  $f$  as

$$a_{\tilde{f}Li}^0 = \sqrt{2}(g_2 I_{3fL} N_{i2}^* + g_Y Y_{fL} N_{i1}^*),$$

$$\begin{aligned}
a_{\tilde{f}_1 Ri}^0 &= y_{f_1} N_{i4}^* , \quad a_{\tilde{f}_2 Ri}^0 = y_{f_2} N_{i3}^* , \\
b_{\tilde{f} Ri}^0 &= -\sqrt{2} g_Y Y_{fR} N_{i1} , \\
b_{\tilde{f}_1 Li}^0 &= y_{f_1} N_{i4} , \quad b_{\tilde{f}_2 Li}^0 = y_{f_2} N_{i3} , \\
a_{\tilde{f}_1 Li}^- &= g_2 V_{i1}^* , \quad a_{\tilde{f}_2 Li}^+ = g_2 U_{i1}^* , \\
a_{\tilde{f}_1 Ri}^- &= -y_{f_1} V_{i2}^* , \quad a_{\tilde{f}_2 Li}^+ = -y_{f_2} U_{i2}^* , \\
b_{\tilde{f}_1 Li}^- &= -y_{f_2} U_{i2} , \quad b_{\tilde{f}_2 Li}^+ = -y_{f_1} V_{i2} , \\
b_{\tilde{f} Ri}^\pm &= 0 .
\end{aligned} \tag{A.10}$$

We next show the explicit forms of the two-point functions  $\Sigma_{0ij}$  and  $\Sigma_{-ij}$  from quark-squark loops. For neutralinos, we have

$$\begin{aligned}
\Sigma_{0ij}^L(p^2) &= \frac{N_c}{16\pi^2} (a_{\tilde{q}ki}^{0*} a_{\tilde{q}kj}^0 + b_{\tilde{q}ki}^0 b_{\tilde{q}kj}^{0*}) B_1(p^2, m_q, m_{\tilde{q}k}) , \\
\Sigma_{0ij}^R(p^2) &= \Sigma_{0ji}^L(p^2) , \\
\Sigma_{0ij}^M(p^2) &= \frac{N_c}{16\pi^2} (b_{\tilde{q}ki}^{0*} a_{\tilde{q}kj}^0 + a_{\tilde{q}ki}^0 b_{\tilde{q}kj}^{0*}) m_q B_0(p^2, m_q, m_{\tilde{q}k}) .
\end{aligned} \tag{A.11}$$

For charginos we have

$$\begin{aligned}
\Sigma_{-ij}^L(p^2) &= \frac{N_c}{16\pi^2} (a_{\tilde{d}ki}^{+*} a_{\tilde{d}kj}^+ B_1(p^2, m_u, m_{\tilde{d}k}) + b_{\tilde{u}ki}^- b_{\tilde{u}kj}^{-*} B_1(p^2, m_d, m_{\tilde{u}k})) , \\
\Sigma_{-ij}^R(p^2) &= \frac{N_c}{16\pi^2} (b_{\tilde{d}ki}^{+*} b_{\tilde{d}kj}^+ B_1(p^2, m_u, m_{\tilde{d}k}) + a_{\tilde{u}ki}^- a_{\tilde{u}kj}^{-*} B_1(p^2, m_d, m_{\tilde{u}k})) , \\
\Sigma_{-ij}^M(p^2) &= \frac{N_c}{16\pi^2} (b_{\tilde{d}ki}^{+*} a_{\tilde{d}kj}^+ m_u B_0(p^2, m_u, m_{\tilde{d}k}) + a_{\tilde{u}ki}^- b_{\tilde{u}kj}^{-*} m_d B_0(p^2, m_d, m_{\tilde{u}k})) .
\end{aligned} \tag{A.12}$$

Here  $B_{0,1}$  are 't Hooft-Veltman functions in the convention of [17].

Finally, we show the corrected  $s$ -channel amplitudes  $i\mathcal{M}_{\tilde{\ell}\tilde{\ell}^*}^{(s)}$  for  $e^-(p_1)e^+(p_2) \rightarrow \tilde{\ell}_i(p_3)\tilde{\ell}_i^*(p_4)$ . In terms of the transverse part of the  $\overline{\text{DR}}$  gauge-boson self-energies,  $\Pi_{\gamma\gamma, \gamma Z, ZZ}^T(s)$ , they are expressed as

$$\begin{aligned}
i\mathcal{M}_{\tilde{\ell}\tilde{\ell}^*}^{(s)} &= + 2ie^2 Q_e Q_{\tilde{\ell}} \left( 1 - \frac{\Pi_{\gamma\gamma}^T(s)}{s} \right) \bar{v}(p_2) \not{p} u(p_1) \\
&+ 2ieg_Z \frac{\Pi_{\gamma Z}^T(s)}{s(s - M_Z^2)} \bar{v}(p_2) \not{p} \left[ Q_e (I_{3\tilde{\ell}} - s_W^2 Q_{\tilde{\ell}}) + (I_{3e} P_L - s_W^2 Q_e) Q_{\tilde{\ell}} \right] u(p_1) \\
&+ 2ig_Z^2 (I_{3\tilde{\ell}} - s_W^2 Q_{\tilde{\ell}}) \frac{1}{s - M_Z^2} \left( 1 - \frac{\Pi_{ZZ}^T(s) - \Pi_{ZZ}^T(M_Z^2)}{s - M_Z^2} \right) \\
&\times \bar{v}(p_2) \not{p} (I_{3e} P_L - s_W^2 Q_e) u(p_1) ,
\end{aligned} \tag{A.13}$$

where  $s = (p_1 + p_2)^2$ ,  $g_Z = g_2/c_W$ , and  $M_Z$  is the  $Z$ -boson pole mass.

## Appendix B: Effective couplings for gauginos

In this appendix, we show how the full one-loop  $t$ -channel amplitudes factorize into a form corresponding to an effective theory. The effective theory amplitude depends on effective couplings,



masses, and mixing matrices. We explicitly show what approximations are necessary for this, and justify them. As a by-product, we show the cancellation of UV divergences in the one-loop amplitudes. Here, for brevity, only the case of  $\tilde{e}_R^- \tilde{e}_R^+$  production is discussed. The generalization to other channels is straightforward.

We first prove that the loop corrected  $t$ -channel amplitude (Eq. (A.5)) can be written in terms of the mass matrix of neutralinos  $Y \equiv Y_N$  in the gauge eigenbasis, instead of the mixing matrix  $N$  and  $m_{\tilde{\chi}_i^0}$ . By substituting Eq. (A.10), Eq. (A.5) takes the form (the  $\Sigma_{ij} \equiv \Sigma_{0_{ij}}$ 's are functions of  $p^2$ )

$$i\mathcal{M}_{RR}^{(t)} = g_Y^2 N_{i1}^* \left[ \frac{\delta_{ij}}{p^2 - m_i^2} - \frac{1}{(p^2 - m_i^2)(p^2 - m_j^2)} (p^2 \Sigma_{ij}^L + m_i m_j \Sigma_{ij}^R + m_i \Sigma_{ij}^M + m_j \Sigma_{ij}^{M*}) \right] N_{j1} X. \quad (\text{B.1})$$

Here we use abbreviations  $m_i = m_{\tilde{\chi}_i^0}$  and  $X = -2iY_{eR}^2 \bar{v}(p_2) \not{p} P_R u(p_1)$ .

At tree-level,  $Y$ , diagonalized masses  $M_D = \text{diag}(m_i)$ , and  $N$  are related by

$$M_D = N^* Y N^\dagger = N Y^\dagger N^T. \quad (\text{B.2})$$

We can transform the tree-level part of Eq. (B.1) as

$$\begin{aligned} N_{i\alpha}^* \frac{1}{p^2 - m_i^2} N_{i\beta} &= \left[ N^\dagger \frac{1}{p^2 - M_D^2} N \right]_{\alpha\beta} \\ &= \left[ N^\dagger \frac{1}{p^2 - N Y^\dagger Y N^\dagger} N \right]_{\alpha\beta} \\ &= \left[ \frac{1}{p^2 - Y^\dagger Y} \right]_{\alpha\beta}, \end{aligned} \quad (\text{B.3})$$

where  $\alpha = \beta = 1$  in this case. The loop corrected part can be written by noting that the two-point functions  $\Sigma$  are given in terms of the gauge eigenbasis functions  $\tilde{\Sigma}$ , as

$$\begin{aligned} \Sigma^L &= N \tilde{\Sigma}^L N^\dagger, \\ \Sigma^R &= N^* \tilde{\Sigma}^R N^T, \\ \Sigma^M &= N^* \tilde{\Sigma}^M N^\dagger. \end{aligned} \quad (\text{B.4})$$

The total  $t$ -channel amplitude is therefore expressed as

$$i\mathcal{M}_{RR}^{(t)} = g_Y^2 \left[ (p^2 - Y^\dagger Y)^{-1} - (p^2 - Y^\dagger Y)^{-1} \left\{ (p^2 \tilde{\Sigma}^L(p^2) + Y^\dagger \tilde{\Sigma}^R(p^2) Y + Y^\dagger \tilde{\Sigma}^M(p^2) + \tilde{\Sigma}^{M*}(p^2) Y \right\} (p^2 - Y^\dagger Y)^{-1} \right]_{11} X, \quad (\text{B.5})$$

Next, we absorb the main loop contributions into an effective neutralino mixing matrix and effective couplings. We define the effective neutralino mass matrix as

$$\bar{Y}(p^2) = Y - \tilde{\Sigma}^M(p^2) - \frac{1}{2} Y \tilde{\Sigma}^L(p^2) - \frac{1}{2} \tilde{\Sigma}^R(p^2) Y. \quad (\text{B.6})$$

The one-loop pole masses  $m_i(\text{pole})$  are obtained from  $\bar{Y}$  as

$$\begin{aligned} m_i(\text{pole}) &= \text{Re}(N^* \bar{Y}(m_i^2) N^\dagger)_{ii} \\ &= m_i - \frac{1}{2} [m_i(\Sigma^L + \Sigma^R)_{ii} + (\Sigma^M + \Sigma^{M*})_{ii}] (m_i^2) , \end{aligned} \quad (\text{B.7})$$

The amplitude Eq. (B.5) becomes, up to  $\mathcal{O}(g_Y^2)$ ,

$$\begin{aligned} i\mathcal{M}_{RR}^{(t)} &= g_Y^2 X \left[ (p^2 - \bar{Y}^\dagger \bar{Y}(p^2))^{-1} \right. \\ &\quad \left. + \frac{1}{2} (p^2 - Y^\dagger Y)^{-1} \tilde{\Sigma}^L + \frac{1}{2} \tilde{\Sigma}^L (p^2 - Y^\dagger Y)^{-1} \right]_{11} . \end{aligned} \quad (\text{B.8})$$

The remaining  $\tilde{\Sigma}_{ij}^L$  have an important property. Their off-diagonal terms are generated by the breaking of  $\text{SU}(2) \times \text{U}(1)$  gauge symmetry in the quark-squark sector, and are UV finite. For sufficiently heavy squarks the contributions of the factors  $\tilde{\Sigma}_{1i,i1}^L (i \neq 1)$  are insignificant and can be dropped. Then, by introducing the effective gaugino coupling

$$\bar{g}_{e\tilde{e}_R\tilde{B}}(p^2) \equiv g_Y \left( 1 - \frac{1}{2} \tilde{\Sigma}_{11}^L(p^2) \right) , \quad (\text{B.9})$$

the  $t$ -channel amplitude is expressed in a very simple form

$$\begin{aligned} i\mathcal{M}_{RR}^{(t)} &\sim \bar{g}_{e\tilde{e}_R\tilde{B}}^2(p^2) [(p^2 - \bar{Y}^\dagger \bar{Y}(p^2))^{-1}]_{11} X \\ &= \left( \frac{\bar{g}_{e\tilde{e}_R\tilde{B}}^2 \bar{N}_{i1}^* \bar{N}_{i1}(p^2)}{p^2 - \bar{m}_i^2(p^2)} \right) X , \end{aligned} \quad (\text{B.10})$$

where  $\bar{m}_i(p^2)$  and  $\bar{N}(p^2)$  are the effective masses and the effective mixing matrix, respectively, obtained by diagonalizing  $\bar{Y}(p^2)$ . Eq. (B.10) takes the same form as the tree-level amplitude Eq. (B.1) with the replacement of the neutralino masses and couplings with the effective ones. It is now evident that the corrected amplitude Eq. (B.1) is UV finite, since both  $\bar{Y}(p^2)$  and  $\bar{g}_{e\tilde{e}_R\tilde{B}}(p^2)$  are finite.

The  $t$ -channel amplitudes for other processes are similarly expressed in terms of effective mass matrices and couplings of neutralinos and charginos. Below we list the forms of other effective lepton-slepton-gaugino couplings which are relevant to our processes:

$$\begin{aligned} \bar{g}_{e\tilde{e}_L\tilde{B}}(p^2) &= g_Y \left( 1 - \frac{1}{2} \tilde{\Sigma}_{011}^R(p^2) \right) , \\ \bar{g}_{e\tilde{e}_L\tilde{W}}(p^2) &= g_2 \left( 1 - \frac{1}{2} \tilde{\Sigma}_{022}^R(p^2) \right) , \\ \bar{g}_{e\tilde{\nu}_e\tilde{W}}(p^2) &= g_2 \left( 1 - \frac{1}{2} \tilde{\Sigma}_{-11}^R(p^2) \right) . \end{aligned} \quad (\text{B.11})$$

Note that the effective couplings are independent of (s)fermion flavor, and hence the  $(\log M_{\tilde{Q}} + \text{const})$  corrections are universal, in analogy with the oblique corrections of the gauge bosons [9, 11].

## References

- [1] The LEP collaborations ALEPH, DELPHI, L3, OPAL, the LEP Electroweak Working Group and the SLD Heavy Flavour Group, preprint CERN-PPE/96-183; J. Ellis, G.L. Fogli and E. Lisi, Phys. Lett. **B389**, 321 (1996); W. de Boer, A. Dabelstein, W. Hollik, W. Mösle, U. Schwickerath, hep-ph/9609209 v4(Nov, 1996); K. Hagiwara, D. Haidt, S. Matsumoto, hep-ph/9706331.
- [2] I. Hinchliffe, F.E. Paige, M.D. Shapiro, J. Soderqvist, W. Yao, Phys. Rev. D **55**, 5520 (1997).
- [3] JLC Group, JLC-1, KEK Report No. 92-16 (1992).
- [4] T. Tsukamoto et al., Phys. Rev. D **51**, 3153 (1995).
- [5] J.L. Feng, M.E. Peskin, H. Murayama, X. Tata, Phys. Rev. D **52**, 1418 (1995).
- [6] M.M. Nojiri, Phys. Rev. D **51**, 6281 (1995).
- [7] H. Baer, R. Munroe, X. Tata, Phys. Rev. D **54**, 6735 (1996).
- [8] M.M. Nojiri, K. Fujii, T. Tsukamoto, Phys. Rev. D **54**, 6756 (1996).
- [9] H.-C. Cheng, J.L. Feng, N. Polonsky, hep-ph/9706438.
- [10] H.-C. Cheng, J.L. Feng, N. Polonsky, hep-ph/9706476.
- [11] L. Randall, E. Katz, S. Su, hep-ph/9706478 and MIT-CTP-2646, inpreparation.
- [12] D.M. Pierce, S. Thomas, SLAC-PUB-7474, in preparation.
- [13] P.H. Chankowski, Phys. Rev. D **41**, 2877 (1990).
- [14] A.G. Cohen, D.B. Kaplan, A.E. Nelson, Phys. Lett. **B388**, 588 (1996).
- [15] W. Siegel, Phys. Lett. **84B**, 193 (1979); D.M. Capper, D.R.T. Jones, P. van Nieuwenhuizen, Nucl. Phys. **B167**, 479 (1980); I. Antoniadis, C. Kounnas, K. Tamvakis, Phys. Lett. **119B**, 377 (1982).
- [16] J.A. Grifols, J. Sola, Nucl. Phys. **B253**, 47 (1985).
- [17] D.M. Pierce, J.A. Bagger, K.T. Matchev, R.-J. Zhang, Nucl. Phys. **B491**, 3 (1997).
- [18] D. Pierce, A. Papadopoulos, Nucl. Phys. **B430**, 278 (1994); D. Pierce, A. Papadopoulos, Phys. Rev. D **50**, 565 (1995).
- [19] J.F. Gunion, H.E. Haber, Nucl. Phys. **B272**, 1 (1986); **B402**, 567 (1993)(E).
- [20] J.L. Feng, T. Moroi, hep-ph/9612333.
- [21] S. Kiyoura, M.M. Nojiri, D.M. Pierce, Y. Yamada, work in progress.

Figure 1: Feynman graphs of the one-loop quarks-squark corrections to the processes  $e^-e^+ \rightarrow \tilde{\ell}\tilde{\ell}^*$ , for (a)  $s$ -channel and (b)  $t$ -channel amplitudes.

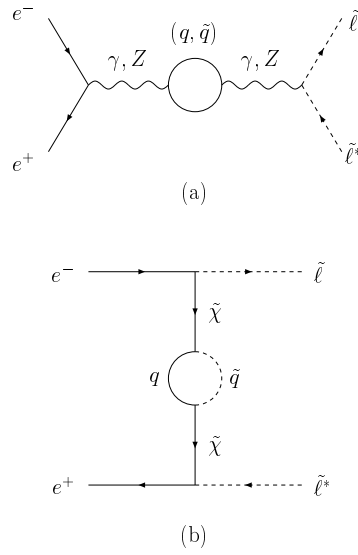


Fig. 1

Figure 2: The dependence of the lowest-order (0) and one-loop (corr) cross-sections of all possible slepton production channels on the  $\overline{\text{DR}}$  renormalization scale  $Q$ . The ratios  $\sigma(Q)/\sigma(Q = M_Z)$  are shown for each channel. Parameters are chosen as  $M_1(M_1) = 100$  GeV,  $M_2(M_2) = 200$  GeV,  $\mu(|\mu|) = -300$  GeV,  $\tan\beta(M_Z) = 4$ ,  $m_{\tilde{\ell}} = 200$  GeV,  $M_{\tilde{Q}} = 1000$  GeV, and  $\sqrt{s} = 500$  GeV.

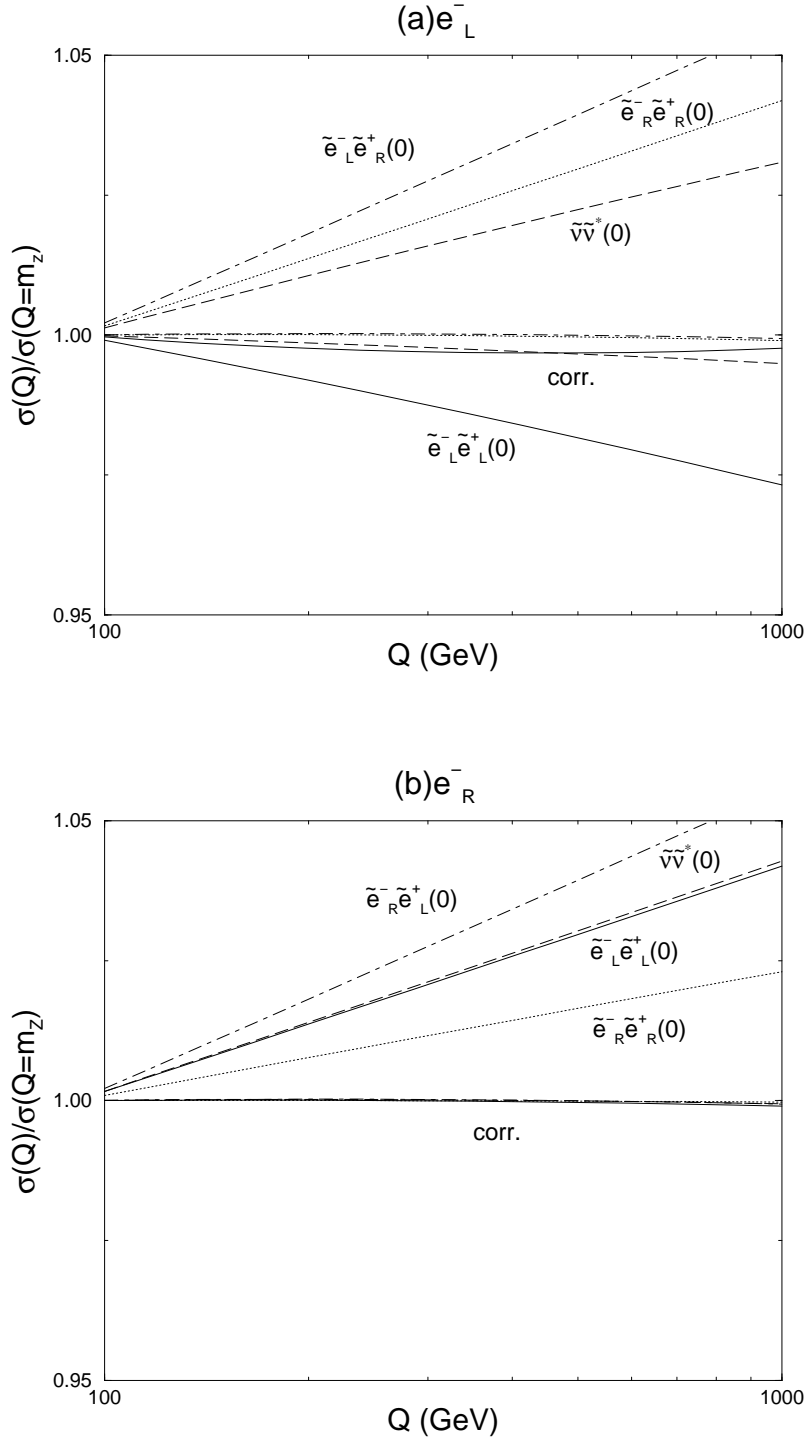


Figure 3: The  $M_{\tilde{Q}}$  dependence of the slepton production cross-sections. Input parameters are  $m_{\tilde{\chi}_1^0} = 100$  GeV,  $m_{\tilde{\chi}_1^\pm} = 200$  GeV,  $m_{\tilde{\chi}_3^0} = 300$  GeV,  $\tan\beta(M_Z) = 4$ ,  $m_{\tilde{\ell}} = 200$  GeV,  $A = 0$ ,  $\mu < 0$ , and  $\sqrt{s} = 500$  GeV. The corrected cross-sections are normalized by the tree-level cross-sections, which are defined in the text.

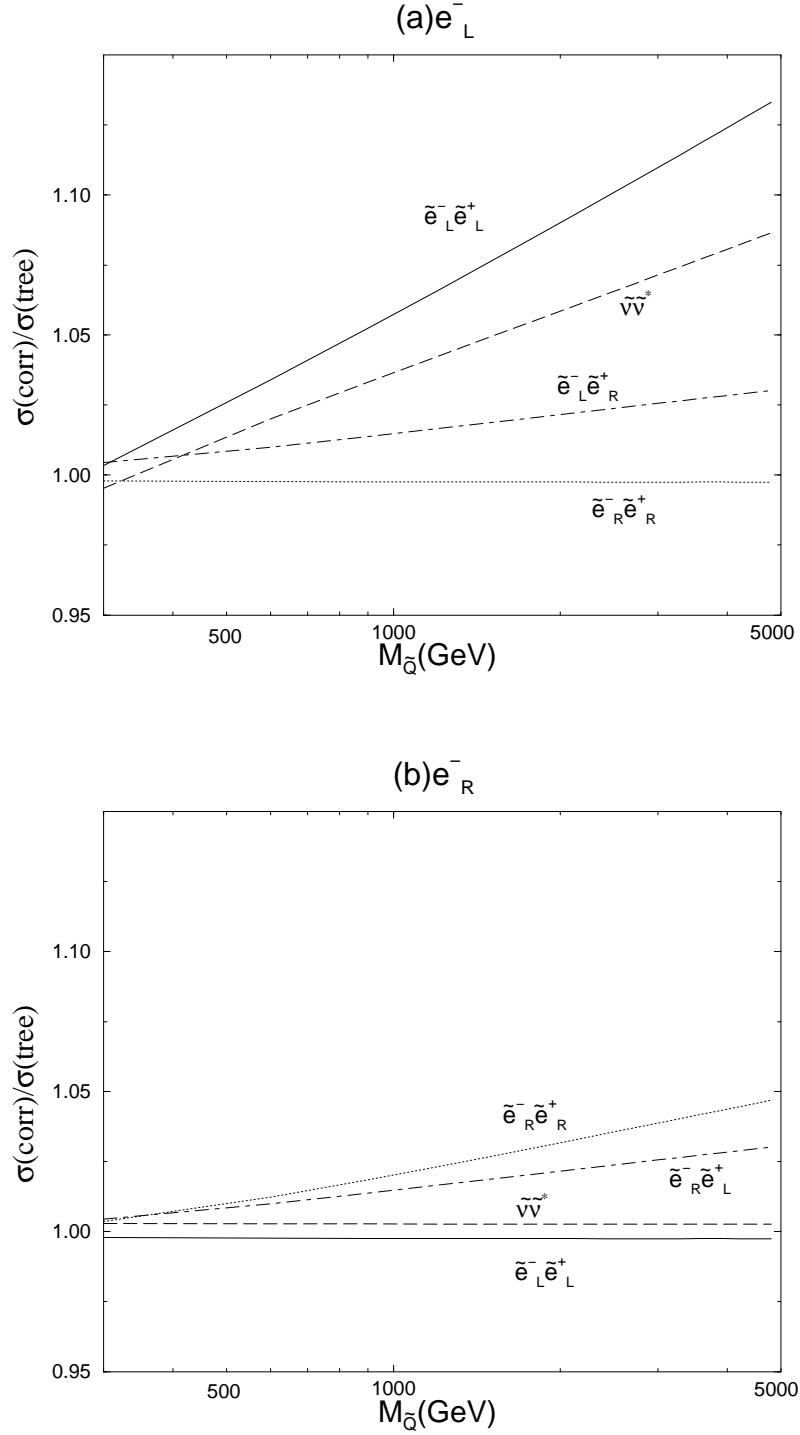


Figure 4: The full corrected cross-sections (solid lines) and two approximations, the effective theory approximation (ETA, dashed lines), and leading log approximation (LLA, dotted with squares), for two channels  $e_L^- e^+ \rightarrow \tilde{\nu}_e \tilde{\nu}_e^*$  and  $e_R^- e^+ \rightarrow \tilde{e}_R^- \tilde{e}_R^+$ , vs.  $M_{\tilde{Q}}$ . The cross-sections are normalized by the tree-level ones, as in Fig. 3. Input parameters are the same as in Fig. 3.

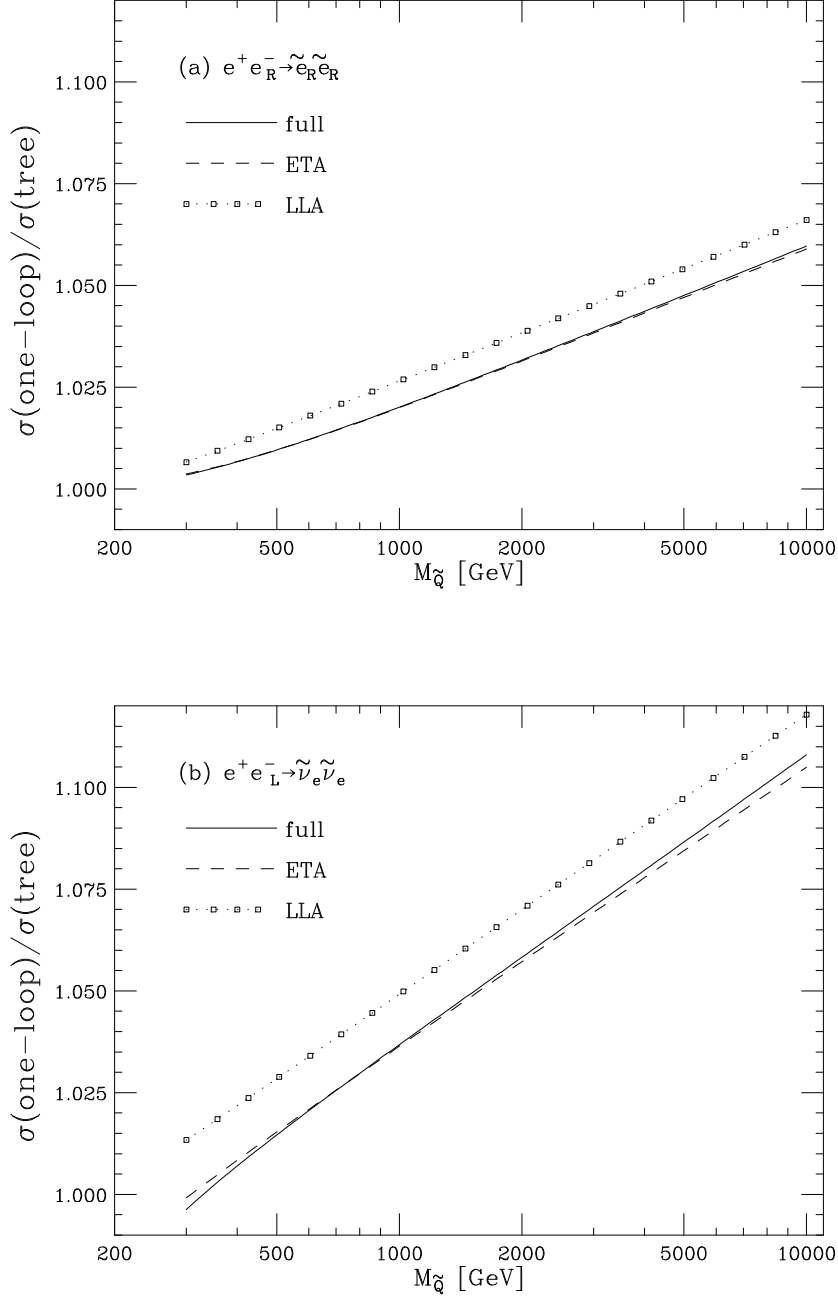


Figure 5: The cross-section  $\sigma(e_L^- e^+ \rightarrow \tilde{\nu}_e \tilde{\nu}_e^*)$  as a function of  $(M_{\tilde{Q}}, A)$ , normalized by the value at  $M_{\tilde{Q}} = 400$  GeV and  $A = 0$ . Input parameters are the same as in Fig. 3, except that  $\tan\beta(M_Z) = 1.5$  and  $\mu$  is either (a) negative or (b) positive. In the black regions a squark is lighter than the  $Z$ -boson.

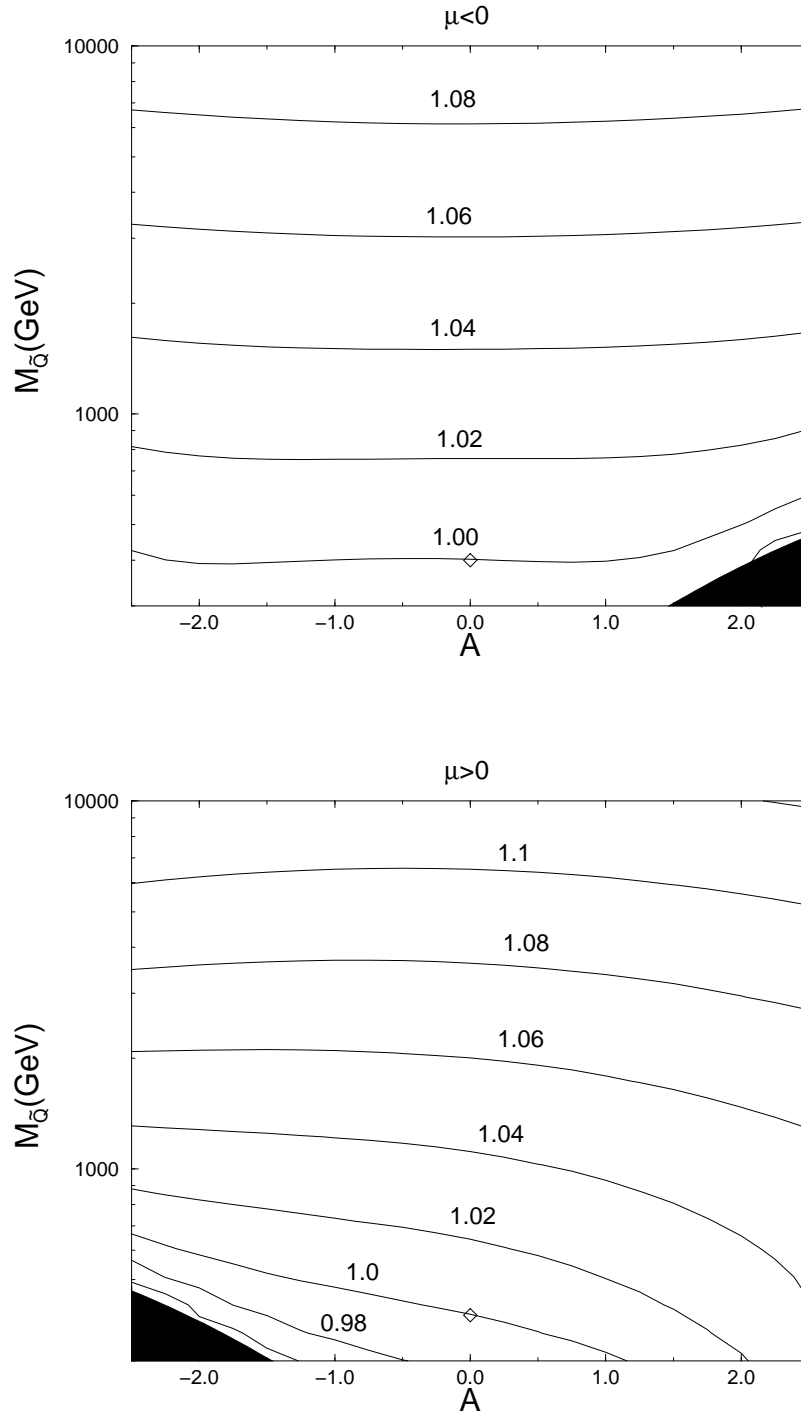




Figure 6: The constraint on  $M_{\tilde{Q}}$  and  $\tan\beta$  coming from  $\sigma(e^-e^+ \rightarrow \tilde{\nu}_e\tilde{\nu}_e^* \rightarrow e^-e^+\tilde{\chi}_1^+\tilde{\chi}_1^-)$ , with  $\int dtL = 100 \text{ fb}^{-1}$ . The central value is taken as  $M_{\tilde{Q}}=1000 \text{ GeV}$  and  $\tan\beta(M_Z) = 4$ . Plotted are the one-loop corrected constant sneutrino production cross-section corresponding to a given number of  $\sigma$  fluctuations from the central value. The masses are fixed and the mass uncertainties are not taken into account. For (a)  $m_{\tilde{\chi}_3^0} = 270 \text{ GeV}$ ,  $\mu < 0$ , (b)  $m_{\tilde{\chi}_3^0} = 270 \text{ GeV}$ ,  $\mu > 0$  and (c)  $m_{\tilde{\chi}_3^0} = 500 \text{ GeV}$ ,  $\mu > 0$ .

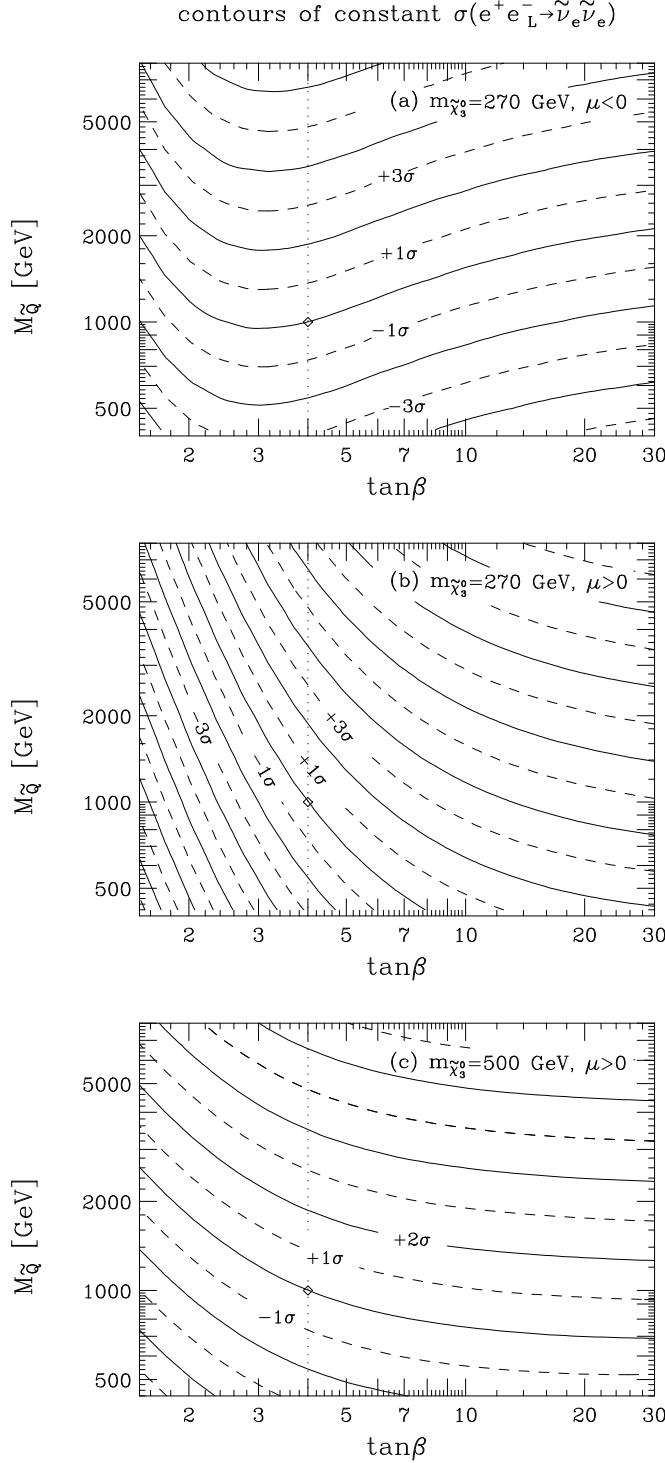


Figure 7:  $\Delta\chi_{\min}^2$  vs.  $M_{\tilde{Q}}$  with  $\mu < 0$  and fixed  $\tan\beta$ ,  $m_{\tilde{\chi}_1^0}$  and  $m_{\tilde{\chi}_3^0}$ , but allowing  $m_{\tilde{\chi}_1^+}$  and  $m_{\tilde{\nu}_e}$  to vary freely. The assumed mass error is  $(\delta m_{\tilde{\chi}_1^+}, \delta m_{\tilde{\nu}_e}) = (0,0)$  for the solid line,  $(0.27 \text{ GeV}, 0.55 \text{ GeV})$  for the dashed line, and  $(0.53 \text{ GeV}, 1.11 \text{ GeV})$  for the short dashed line. The mass errors for the short dashed line are obtained by statistically scaling up the results of Ref. [7] from  $20 \text{ fb}^{-1}$  to  $100 \text{ fb}^{-1}$ .

